JIMMA UNIVERSITY

COLLEGE OF NATURAL SCIENCES

SCHOOL OF GRADUATE STUDIES

DEPARTMENT OF CHEMISTRY

MSc THESIS

SYNTHESIS OF ZnO NANOPARTICLES USING *LEPIDIUM SATIVUM* SEED EXTRACT FOR PHOTOCATALYTIC AND ANTIMICROBIAL STUDIES

By

BUZUNESH TEMESGEN

JANUARY, 2021

JIMMA, ETHIOPIA

SYNTHESIS OF ZnO NANOPARTICLES USING *LEPIDIUM SATIVUM* SEED EXTRACT FOR PHOTOCATALYTIC AND ANTIMICROBIAL STUDIES

A THESIS SUBMITTED TO SCHOOL OF GRADUTE STUDIES, JIMMA UNIVERSITY IN PARTIAL FULFILMENT OF THE REQUIRMENTS FOR THE DEGREE OF MASTER OF SCIENCE IN CHEMISTRY (INORGANIC CHEMISTRY)

By

BUZUNESH TEMESGEN

PRINCIPAL ADIVISOR: GUTA GONFA (PhD)

CO-ADVISOR: KIRUBEL TESHOME (Assi. prof)

JANUARY, 2021

JIMMA, ETHIOPIA

JIMMA UNIVERSITY SCHOOL OF GRADUATE STUDIES COLLEGE OF NATURAL SCIENCES DEPARTMENT OF CHEMISTRY

SYNTHESIS OF ZnO NANOPARTICLES USING *LEPIDIUM SATIVUM* SEED EXTRACT FOR PHOTOCATALYTIC AND ANTIMICROBIAL STUDIES

By

BUZUNESH TEMESGEN

APPROVED BY BOARD OF EXAMINERS

Principal Adviser	**Signature**	**Date**
_____	_____	_____
Co-Adviser		
_____	_____	_____
Internal Examiner		
_____	_____	_____
External Examiner		
_____	_____	_____
Chair person		
_____	_____	_____

JANUARY, 2021

JIMMA, ETHIOPIA

TABLE OF CONTENTS

Contents

LIST OF FIGURES

Figure **page**

LIST OF TABLES

Table **page**

ABBREVIATIONS AND ACRONYMS

Å	Angstrom
DMSO	Dimethyl Sulfoxide
eV	Electron Volt
FTIR	Fourier Transform Infrared spectroscopy
mM	Millimolar
MO	Methyl orange
PXRD	Powder X-ray Diffraction
UV-vis spectroscopy	Ultraviolet Visible spectroscopy
ZnO-NPS	Zinc Oxide Nanoparticles

ACKNOWLEDGEMENT

First of all, I would like to thank the Almighty GOD for giving me strength and wisdom to develop this thesis. Next, I would like to offer my deepest gratitude to my advisors, Dr. Guta Gonfa and Mr. Kirubel Teshome for their valuable guidance, support, advices, encouragements, constructive comment, unreserved cooperation and fatherly helps throughout the work.

I am thankful to Department of Chemistry, Jimma University for the material support and giving me access to all laboratory facilities for this study and laboratory technicians for their cooperation in giving information on the availability of some apparatus. I am thankful to college of agriculture and veterinary medicine for bioassay study, Jimma University. I am also thankful for Chemistry Department of Addis Ababa University for their great support in spectroscopic Analysis of the sample. I would like to express my deepest gratitude to Mr. Addismiraf Alemu his encouragement during the course of the study.

Finally, I would like to express my deepest thank to my family specially my mother Mrs. Kassech Worku and my sister Miss Bereket Temesgen for their financial, moral supports and encouragements throughout this study.

ABSTRACT

Environmental pollutants are one of the most series global issues today. Dyes are recognized as one of the roots for environmental pollution. Methyl orange (MO) are a type of dyes which can be found in various branches of textile, leather, and paper printing industries. In recent years, microbial infections are considered as a serious issue in human health worldwide. The advancement of nanotechnology based on bio-synthesis of medicinal plant supported nanoparticles has improved therapeutic capacity of ZnO nanoparticles. The main objective of this study was to synthesize ZnO nanoparticles using *Lepidium sativum* seed extract for their photocatalytic and antibacterial activities. The plant mediated synthesized ZnO nanoparticles was prepared from macerated extract of *Lepidium sativum* seeds, zinc acetate dihydrate and sodium hydroxides at room temperature. The synthesized ZnO nanoparticles were characterized by UV-Vis, FT-IR spectroscopic techniques and Powder XRD analysis. The color change observed in the nanoparti cle's solution and the sharp peak at 376 nm in the UV–Vis region suggested that the formation of small-sized ZnO nanoparticles. The color changed during the preliminary phytochemical investigation and the FT-IR spectroscopic analysis suggested the presence of flavonoids, tannin, saponin and Alkaloids which could be responsible for the stabilization of the synthesized ZnO nanoparticles. The XRD studies the synthesized zinc oxide nanoparticles has crystalline size of 29 nm which predict as hexagonal structure. The photocatalytic activity of MO dye degradation was efficient in the presence ZnO nanoparticle catalyst as compared to in the absence of ZnO nanoparticle catalyst. Finally, the bio-assay test showed 13 to 24 zone of inhibition for zinc oxide nanoparticles and 11 to 16 zone of inhibition for plant extract against different bacterial strains. The highest activity was observed against *Klebsiella* for zinc oxide nanoparticles compared to plant extract alone, which might be due to synergistic effect.

Key words: *ZnO-Nanoparticles, Lepidium sativum, phytochemicals, Methyl orange, Photocatalytic activity, Antibacterial activity*

1. INTRODUCTION

1.1 Background of the study

Nowadays, a vast amount of toxic effluents is discharged to the environment through the rapid industrialization [1]. A number of industries such as leather, paper, plastic, textile, food processin g, printing, cosmetics and pharmaceuticals, etc., deal with the aid of dyes. In addition to these, some of the dyes can cause serious health problems such as mutation and cancer [2]. Other industries produce a large number of organic contaminants including dyes which are toxic and non biodegradable. The presence of these contaminants causing severe environmental pollution problems by the releasing toxic and potential carcinogenic substances into the aqueous phase [3].

Methyl orange is an anionic dye having molecular formula[$C_{14}H_{14}N_3NaO_3S$] with molecular of 327.34 g mol^{-1} and maximum absorption wavelength (λ_{max}) at 465 nm [4]. These dyes are widely used in textiles, food, paper, and leather industries, and used as a pH indicator. Due to its toxicity, it produces serious health risks such as cancer, genetic mutation, and biodegradation in humans and animals [5].

Nanoparticles (NPs) are particles which exist the dimensions in the range of 1–100 nm, acting as a bridge between bulk materials and atomic or molecular structures. They have remarkable and interesting properties due their small sizes, large surface area with free dangling bonds and higher reactivity over their bulk cousins [6]. Nanoparticles have both chemical and physical differences in their properties (e.g. mechanical properties, biological and sterical properties, catalytic activity, thermal and electrical conductivity, optical absorption and melting point) compared to bulk of the same chemical composition. Therefore, design and production of materials with novel applications can be achieved by controlling shape and size at nanometer scale [7].

Metal oxide nanoparticles due to their smaller size have properties different than those in the bulk. The physico-chemical properties of metal oxides have special relevance in chemistry mostly related to the industrial use of oxides as sensors, ceramics, adsorbents and catalysts [8]. Physical methods such as adsorption and chemical methods such as chlorination and ozonation are some of the most frequently used methods for the removal of textile dyes. Flocculation and reverse osmosis are also some other methods commonly used, but these methods are not destructive. They just transfer the contaminants from one phase to another for which further treatments are required.

But, advanced oxidation process (AOP) like heterogeneous photocatalysis is a promising technology for water purification going on the surface of photocatalyst under irradiation of photons, leading to total mineralization of dyes [3]. The present study focuses on the design of Zinc oxide (ZnO) nanoparticles has been considered as an essential semiconductor having a wide band gap of 3.37 eV and large exciton binding energy of 60 meV; a highly multitasking metal oxide due to its distinctive electrical and optical properties. Specifically, ZnO efficiently absorbs ultraviolet (UV) light and has surface electrical properties sensitive to the environment at the interface. ZnO, has attracted extensive attention as a photo catalyst for the degradation of organic pollutants in water and air under UV irradiation [9]. ZnO is more efficient in the photodegradation of organic compounds under UV-light illumination. The photocatalytic activity of ZnO nanocrystals is mainly dependent on the type and concentration of the oxygen defects. Therefore, expected to control the nanostructures (e.g., size, morphology, and oxygen defects) of ZnO by using different techniques, thereby tailoring the properties [10].

Many different semiconductor materials, such as TiO, ZnO, ZrO, SrO, Fe_2O_3, CdS, used to photo-degrade different pollutants. Among these, ZnO is known to be the best photo-catalysts for the degradation of several environmental contaminants due to having high band gap energy [5].
ZnO nanoparticles show antibacterial activity against a broad spectrum of pathogenic bacteria, and these nanoparticles adopt various mechanisms such as reactive oxygen species (ROS) generation, cell membrane integrity disruption, biofilm formation, or enzyme inhibition. There are many conventional zinc oxides (ZnO) nanostructure synthesis routes employing the chemical and physical methods, which require particular set-up, high cost, high temperature-pressure conditions, and nonecological chemicals. However, high-energy consumption of these routes and released toxic chemicals after the process can be hazardous to the environment and human health. In recent

years, the green synthesis approach has been gaining attention, which eliminates the use of toxic chemicals and applies environmentally friendly routes [11]. The biosynthesis may actually provide nanoparticles of a better-defined size and morphology as compared to some of other physicochemical methods of production. It has been found that the microbial-based synthesis process is readily scalable, eco-friendly, and compatible with the use of product for pharmacological applications, but production through microorganisms is often more expensive than the production of plant-based materials. The main benefit of plant-based synthesis approaches over classical chemical and physical method is more eco-friendly, cheaper, and easily scale-up process for the large-scale synthesis of nanoparticles with no need to use high temperature, pressure, and toxic chemicals [12].

Medicinal plants are the cheap and safe alternative sources for the prevention against antimicrobial infections. *Lepidium sativum* plant and seeds are considered as one of the popular medicinal herbs used in the community of Saudi Arabia, Sudan and some other Arabic countries as a good mediator for bone fracture healing in the human skeleton [13]. *Lepidium sativum*. Linn (Garden cress) is locally known as "fetto", which belongs to the family of Brassicaceae. It is commonly grown in Ethiopia as a garden plant and found in any market, while usually in small quantities. Commonly used in folk medicine for the treatment of hyperactive airways disorders, such as asthma, bronchitis and cough. About 150 species are found in the temperate and sub temperate areas. Among those species, the present study has been focused on *Lepidium sativum* seed extract [14].

Some researches were done on plants mediated synthesis of ZnO NPs by using some plants like *Leucas aspera, olea europaea* and *Ricinus communis*. However, no work has been reported on *Lepidium sativum* plant seed extract mediated ZnO NPs synthesis. The medicinal usage of the plant traditionally, as well as its healing ability may give a clue about the richness of the plant in phytochemicals. In view of these observations, it is planned to study the removal of methylene orange dye via photocatalytic degradation and evaluation of antibacterial activities of ZnO nanoparticles synthesized using *Lepidium sativum* seed extract.

1.2 Statement of the problem

Traditionally, peoples have been using different plants for the treatment of various diseases without detailed scientific information. *Lepidium sativum* is one of the prominent plants that are traditionally used as antimicrobial agents in numerous areas.

The bioactivities of these plants proved particularly traditionally can be enhanced when the phenolic compounds of the plant extract support the formation and stability metal oxide nanoparticles due to enhancement of penetrating the cell of the pathogens.

On the other hand, metal oxide nanoparticles play a great role in removal of toxic dyes to maintain environmental safety. However, the physical and chemical methods of synthesis of metal oxide nanoparticles are expensive and not eco-friendly. Metal nanoparticles synthesis using plant extract based on green chemistry perspectives impose limited hazards to the environment. In this study, *Lepidium sativum* supported zinc oxide (ZnO) nanoparticles said to have secondary metabolites such as, flavonoids, tannins and alkaloids in its crystal lattice, acting as efficient stabilizing and capping agent was synthesized. Based upon the above evidences, the present study was intended to explore the photocatalytic activity of *Lepidium sativum* seed extract supported zinc oxide (ZnO) NPs and evaluation of their antibacterial activities.

Therefore, this research might answer the following basic questions: -

- How efficient were the *Lepidium sativum* plant seed extract in acting as capping and stabilizing agent for zinc oxide (ZnO) NPs formation?
- In what extent the antimicrobial activity of *Lepidium sativum* is improved with synthesis of zinc oxide (ZnO) NPs?
- How efficient is the *Lepidium sativum* plant extract supported zinc oxide (ZnO) NPs in removing methylene orange dyes?

1.3 Objectives of the study

1.3.1 General objective of the study

The main objective of this study was to synthesize Zinc oxide nanoparticles using *Lepidium sativum* seed extract and evaluate its photocatalytic and antibacterial activity.

1.3.2 Specific objective of the study.

- To prepare seed extract of *Lepidium sativum*.
- To conduct phytochemical screening test of crude extract and characterize by FT-IR spectroscopy.
- To synthesize zinc oxide nanoparticles using the seed extract of *Lepidium sativum*.
- To characterize the synthesized zinc oxide nanoparticles using UV-vis, FT-IR and XRD spectroscopic techniques.

- To explore photocatalytic degradation of methylene orange using zinc oxide nanoparticles.
- To test and compare the antibacterial activity of the plant extract and the synthesized zinc oxide nanoparticles.

1.4 Significance of the study

The green synthesis of metal oxide nanoparticles using a plant extract for varies environmental and medicinal applications are an active area of research, attracting the interest of many researchers globally. Hence, the result of this study may be used as a benchmark of reference for further study on design and application of metal oxide nanoparticles. Furthermore, similar work was done by other stakeholders for application of the metal oxide nano-composites to increase their biological and photocatalytic activities.

2. REVIEW OF RELATED LITRATURES

2.1 Nanotechnology and Nanomaterials

Nanotechnology is a field of science and technology which deals with production, manipulation and use of materials carrying in nanometers. The advances in nanotechnology have led to the greater development in various fields, including nanoparticles, nanotubes, and nanowire synthesis. Nanoparticles (NPs) are natural or anthropogenic materials having at least dimensions between 1–100 nm. NPs possess numerous distinctive properties like high reactivity; unique optical properties and biocompatibility in comparison to their bulk counterparts due to their very high surface area to volume ratio, this shows the difference in their physical and chemical properties [15].

The properties of the NPs influence their behavior, particularly; morphological properties like shape and size can influence NPs circulation and targeting within the body. Nanotechnology plays an important role in the modern research. This technology could be applicable in a wide range of fields such as all pharmacology, food and nutrition, chemical industries, energy sciences, cosmeti cs; further, it can be used for the treatment of infections, cancer, allergies, diabetes and inflamma tion [16].

Despite this fact, nanomaterials have the following limitation or challenges: stability in a hostile environment, lack of understanding in fundamental mechanism and modeling factors, bioaccumulation/ toxicity features, expansive analysis requirements, the need for skilled operators, problem in devices assembling and structures, and recycle/reuse/regeneration. In the true world, it is desirable that the properties, behavior, and types of nanomaterials should be improved to meet the aforementioned points [17].

2.2 Botanical information of *Lepidium sativum*

Medicinal plants are the cheap and safe alternative sources for the prevention against antimicrobial infections. Among those plants, *Lepidium sativum* L. in English, it is called "Garden cress", and locally known as "fetto" (Figure 1) which belongs to the family, Brassicaceae. About 150 species are found in the temperate and sub temperate areas [18]. The traditional uses of *Lepidium sativum* seeds extract are controlling many clinical problems. The aerial parts are used in the treatment of asthma, cough and bleeding piles [19]. *Lepidium sativum* seed extract is known to have antioxidant, antimicrobial, antifungal, anticancer and anti-inflammatory results from the presence of secondary metabolites components (α-tocopherol and

β-sitosterol) [20]. This study was intended to evaluate the *Lepidium sativum* seed extracts supported ZnO NPs as antibacterial activity against some selected pathogenic bacterial strains.

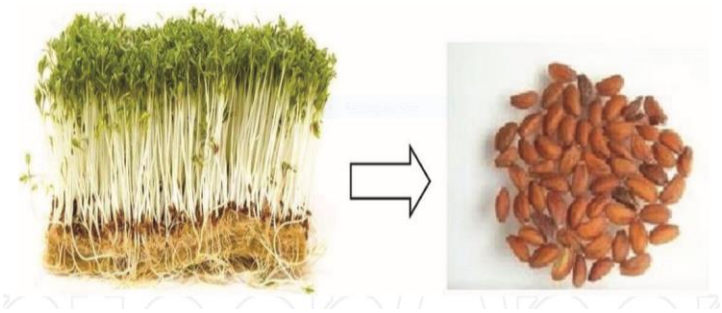

Figure 1. Plants and seeds of *Lepidium sativum* (Garden cress)

2.3 Phytochemical constituents of *Lepidium sativum*

Plants produce a large variety of secondary product that contains a phenol group- a hydroxyl functional group on an aromatic ring. The derivatives of phenolic compounds include simple phenyl propanoid; benzoic acid derivatives, anthocyannin, isoflavones, tannins, lignin, and flavonoid compound beginning with phenyl alanines. Flavonoids are a family of natural polyphenolic compounds that include flavone, flavonol, flavanone, flavanonol, and isoflavone derivatives. The basic function of the flavonoids is for pigmentation and defense. The participation of sugars, terpenoids, polyphenols, alkaloids, phenolic acids, and proteins in the reduction of metal ions into NPs and in supporting their subsequent stability has also been postulated [21].

Large varieties of secondary metabolites have nitrogen in their structure these include the alkaloids, cyanogenic glucoside, and glucosinate. The nitrogen atom in these substances is usually part of the heterocyclic ring, a ring that contain both nitrogen and carbon atom. Alkaloids were once thought to be nitrogenous wastes. Most alkaloid is now believed to function as defense against especially mammals, because of the general toxicity and deterrence capacity [22]. *Lepidium sativum* seed contains the seven imidazole alkaloids, sinapin, and sinapic acid in seeds. It also contains glucotropaeoline, N, N'- Dibenzyl urea, N, N'- Dibenzylthiourea, Sinapic Acid and its choline esters (sinapin), carotene, cellulose, calcium, phosphorus, iron, thiamine, riboflavin, niacin, carotene, uric acid [20] as shown in (Figure.2).

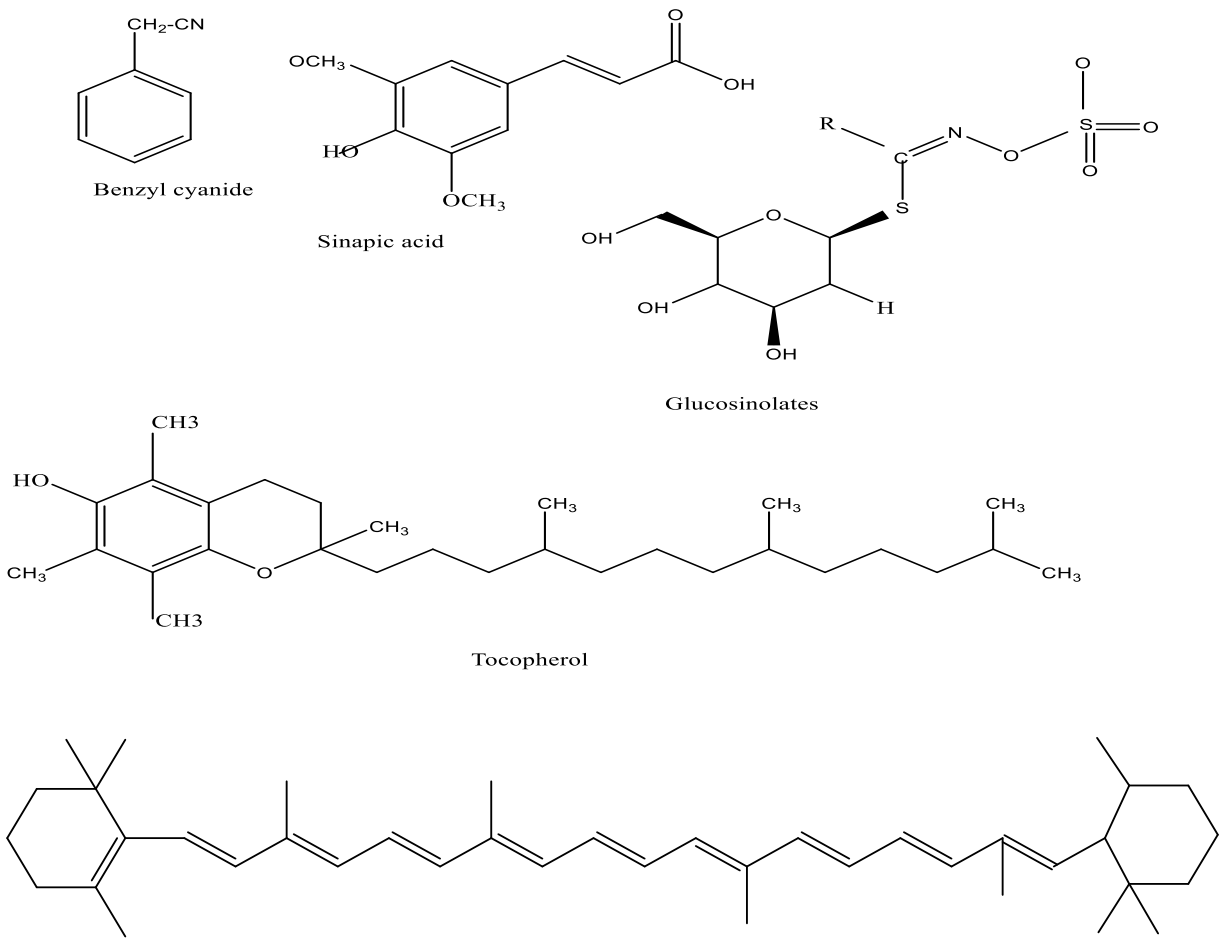

Figure 2. Chemical Structure of some Phytochemicals present in *Lepidium sativum* Linn

2.4 Synthesis method of metal oxide nanoparticles

In classical, nanomaterials are synthesized through; two basic approaches the first approach is the "top-down". In this approach, many physical, chemical and thermal techniques are used to provide the necessary energy for nanoparticles formation and the second approach, known as "bottom-up". In the up-down approach, which is costlier to implement, it is impossible to obtain perfect surfaces and edges due to cavities and roughness that can occur in nanoparticles; whereas excellent nanoparticle synthesis results can be obtained by bottom-up approach. In addition, with the bottom up approach, no waste materials that need to be removed are formed, and nanoparticles having smaller size can be obtained thanks to the better control of sizes of the nanoparticles [23].

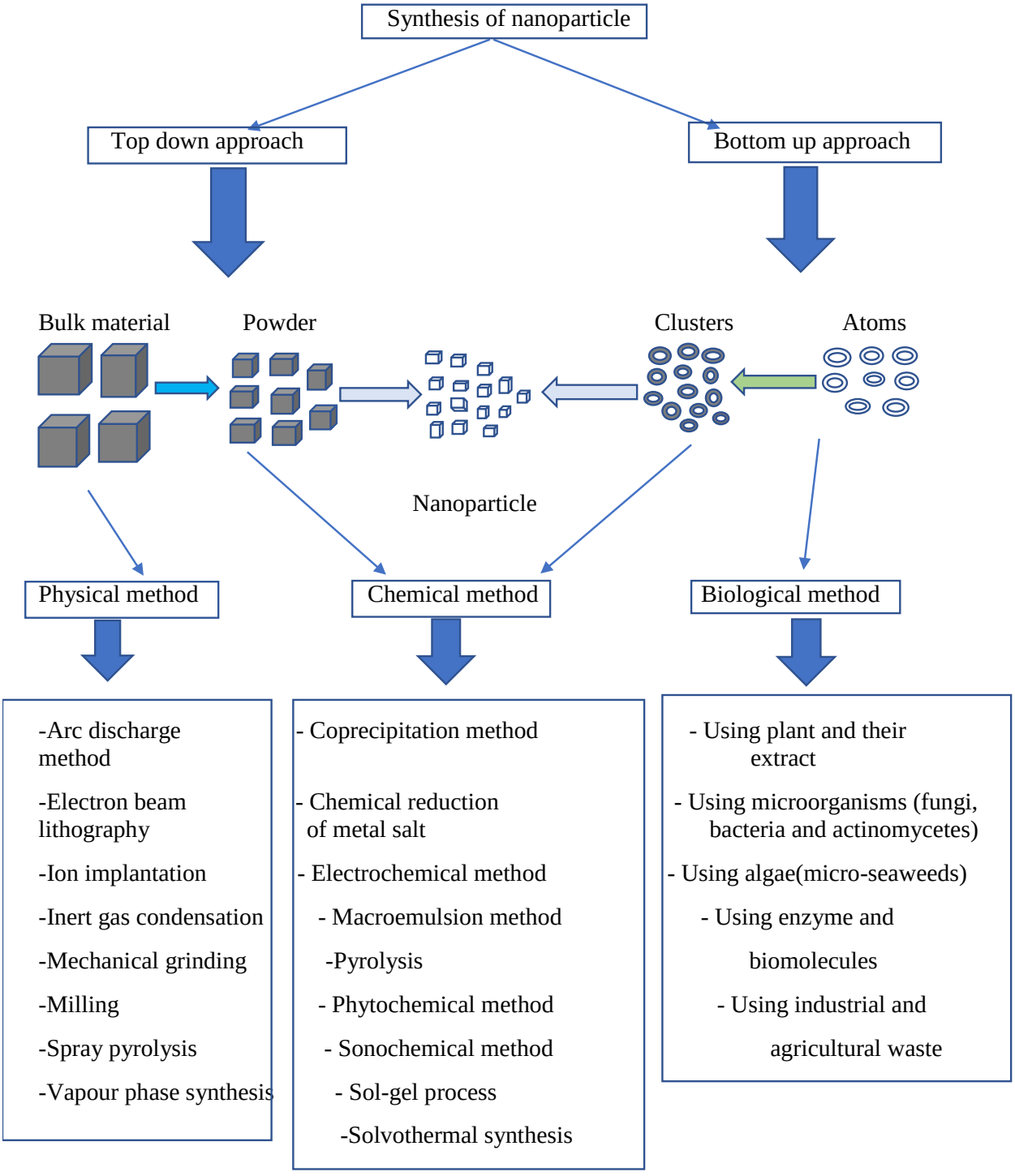

Scheme:1 Approaches and methods in the synthesis of nanomaterials.

Nanoparticles can be synthesized using a variety of methods, including chemical, physical, hybrid and biological technique. Chemical and Physical methods have been using high radiation and highly concentrated registrants' and stabilizing agents that are harmful for the environment and to human health. Hence, biological synthesis of nanoparticles is a single step bioreduction m ethod and less energy is used to synthesize ecofriendly [24].

In traditional chemical and physical methods; reducing agents involved in the reduction of metal ions, and stabilizing agents used to prevent undesired agglomeration of the produced nanoparticles carry a risk of toxicity to the environment and to the cell. Besides, the contents of the produced nanoparticles are thought to be toxic in terms of shape, size and surface chemistry. In the green synthesis method in which nanoparticles with biocompatibility are produced, these agents are naturally present in the employed biological organisms. The biological method, which is represented as an alternative to chemical and physical methods, provides an environmentally friendly way of synthesizing nanoparticles. Moreover, this method does not require expensive, harmful and toxic chemicals. Metallic nanoparticles with various shapes, sizes, contents and physicochemical properties can be synthesized thanks to the biological method actively used in recent years [25].

2.5 Characterization Techniques

UV-visible spectroscopy is used to confirm the formation of various types of nanoparticles by measuring plasmon resonance and evaluating the collective oscillations of conduction band electrons in response to electromagnetic waves. This provides information about the size, structure, stability, and aggregation of the nanoparticles. Metal nanoparticles are associated with specific absorbance bands in characteristic spectra when the incident light enters into resonance with the conduction band electrons on the surface of the nanoparticles [6].

FT-IR Spectroscopy is used to determine the nature of functional groups or metabolites present on the surface of NPs which might be responsible for reduction and stabilization of NPs [26]**.** A recorded spectrum gives the position of bands related to the strength and nature of bonds, and specific functional groups, providing this information concerning molecular structures and interactions [25].

XRD is used to assess the crystallinity of synthesized nanoparticles. This technique is employed to identify and quantitatively examine various crystalline forms or the elemental composition of natural and manufactured materials or nanoparticles [27].

PXRD pattern gives information about translational symmetry, size and phase identification of metallic NPs [27]. The average Crystallite size, D, can be calculated using the well-known Scherrer's equation:

$$D_{hkl} = (k*\lambda) / (\beta_{hkl}* \text{Cos } \theta_{hkl})$$

Where, D_{hkl} is the Crystallite size perpendicular to the normal line of (hkl) plane, k is a constant (0.94), β_{hkl} is the full width at half maximum of the (hkl) diffraction peak, θ_{hkl} is the Bragg angle of (hkl) peak and λ is the wavelength of X-ray.

2.6 Photocatalytic applications of ZnO nanoparticles

Photocatalytic degradation of organic pollutants is a promising approach for the removal of dyes in wastewaters. ZnO nanoparticles have been involved in photocatalytic applications due to their optical and electronic properties. When the ZnO nanoparticles are irradiated with UV light, valence band electrons are excited to the conduction band, which leaves holes behind. Then the generated holes create hydroxyl radicals by oxidizing H_2O and OH^- and the excited electrons are captured by oxygen in the air. The resulting anionic radicals are highly reactive and degrade the organic dyes in to carbon dioxide and water [28].

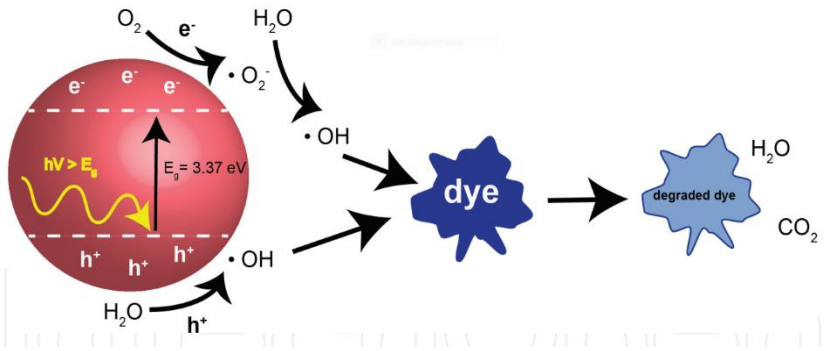

Figure.3 Schematic diagram of dye degradation by ZnO nanostructures.

Zinc oxide (ZnO) is a promising candidate as a photocatalytic material since it exhibits higher photocatalytic efficiencies for the degradation of organic contaminants compared to other metal oxides owing to their high catalyst surface area important factor to enhance photocatalytic activity of metal oxides. Larger effective surface area leads to a higher adsorption of organic molecules leading to a better photocatalytic activity [29]. For a photocatalyst, as the particle size decreases, surface area increases and the number of active sites increases which leads to high reactivity. As the number of active sites increases, the absorbance of pollutants on the surface of the catalyst increase. In photocatalysis degradation takes place when the photocatalyst adsorbs photons of energy greater than its band gap energy [1].

2.7 Antimicrobial activity of metal oxide nanoparticles

Metal oxide nanoparticles are of great interest for use as potential antimicrobial agents because of their unique optical, electronic, and magnetic properties. The electrostatic interaction of nanoparticles with negatively charged bacterial surfaces draws the particles to the bacteria and promotes their penetration into the membrane. A strongly positive zeta potential of a nanoparticle promotes nanoparticle interactions with cell membranes leading to membrane disruption, bacterial flocculation, and a reduction in viability. The generation of reactive oxygen species is also a mechanism of nanoparticle antibacterial activity. Further mechanisms of action of nanoparticles as antimicrobial agents include disrupting deoxyribonucleic acid during the replication and cell division of microorganisms, compromising the bacterial membrane integrity via physical interactions with the microbial cell (the physical presence of a nanoparticle most likely disrupts cell membranes in a dose-dependent manner), and releasing toxic metal ions and possessing abrasive properties which bring about lysis of cells[30] .

The ZnO nanoparticles show antibacterial activity against a broad spectrum of pathogenic bacteria, and these nanoparticles adopt various mechanisms such as reactive oxygen species (ROS) generation, cell membrane integrity disruption, biofilm formation, or enzyme inhibition [31]. Under UV irradiation, ROS such as superoxide ions, hydroxyl ions, singlet oxygen species, and peroxide molecules are formed. The formed peroxide ions could easily penetrate through the cell membrane and result in cell death. Figure 5 shows the possible ROS generation mechanism and its effect on the bacterial cell wall.

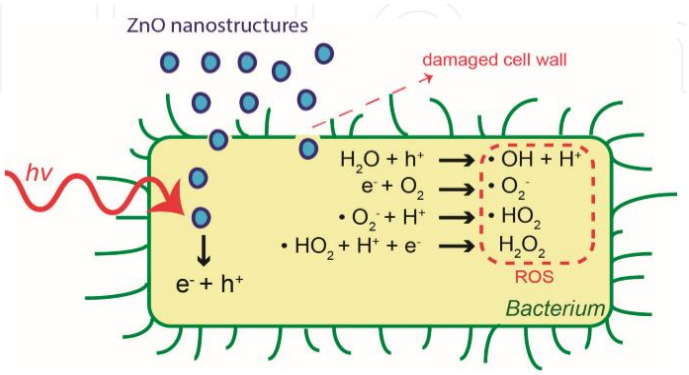

Figure 4. ROS mechanism of ZnO nanoparticles [31].

3. MATERIALS AND METHODS

3.1 Chemicals

Zinc acetate dihydrate Zn $(CH_3COO)_2.2H_2O$, 0.1 M and 2 M Sodium hydroxide (NaOH), Methyl orange (MO), 0.1 M HCl (hydrochloric acid), distilled water, ferric chloride ($FeCl_3$), Potassium iodide (KI) and iodine(I) and DMSO (dimethyl sulfoxide).

3.2 Apparatus and Instruments

Test tube, glass beaker, round bottom flask, heating mantel, magnetic stirrer, thermometer, a mortar, balance, Refrigerator, Conical flask, measuring cylinder, Petri dishes, PH indicator and centrifuges. Ultraviolet visible spectroscopy (UV-Vis) (Aspect - 1.2.3.6173, Analytic jena and UV-Jenway6705), Fourier transform infrared (FTIR) spectroscopy (65 FTIR Perkin Elmer) and Powder X-ray Diffraction (PXRD) diffractogram (Rigaku miniflex600 XRD machine).

3.3 Preparation of the *Lepidium sativum* seeds

Lepidium sativum seed was collected from the local markets of merkato town at jimma zone, Oromia regional state, Ethiopia in January 2019. Then the sample were stayed at room temperatures in Jimma university Inorganic research laboratory.

3.3.1 Extraction of *Lepidium sativum* seeds

5 g of *Lepidium sativum* seeds powder were immersed in 500 mL distilled water and stirred at 70 °C for about 4 h. The mixture was incubated for 3 days at room temperature. The obtained solution was filtered (what man No.1 filter paper) and centrifuged at 6000 rpm. The obtained extract was stored in a dry place (refrigerator) until use [19].

3.4 Phytochemical screening test and characterization of the extract

Flavonoids: To check the presence of flavonoids, 2 mL of sodium hydroxide was added in 2 mL of aqueous extract [32].

Tannin: The presence of tannins was tested by adding 2 mL of 5 % $FeCl_3$ to 2 mL of extract [33].

Saponins: About 1 mL of solvent extract was introduced into a tube containing 1 mL of distilled water, the mixture was vigorously shaken for 2 min [32].

Alkaloids: a drop or two of Wagner's reagent (iodine and potassium iodide) were added to 2 mL of extract for the checkup of this phytochemical's presence [33].

Phenolic: 1 mL of 1% ferric chloride solution was added to 2 mL of extract to test the presence of phenolic phytochemicals [33].

3.5 Synthesis of ZnO nanoparticles using *Lepidium sativum* extract

0.5 g of Zinc acetate dihydrate Zn $(CH_3COO)_2.2H_2O$ was dissolved in 50 mL of distilled water, then 7 mL of this solution was taken and added to 7 mL of the prepared seed solution. The mixture was mixed well using a magnetic stirrer. After a few minutes, 2M NaOH solution was added drop by drop to adjust a pH between10 - 12, due to formation of colloidal almost instantaneously. The mixture was stirred well with the magnetic stirrer for one hour and then kept undisturbed till the colloidal suspension settled down. The colloidal suspension was then collected while discarding the supernatant. This suspension was kept in open air till all the water is evaporated. The obtained product was used for further studies [34].

3.5.1 Optimization of various physicochemical parameters for ZnO NPs synthesis

Physicochemical parameters regulate the green synthesis of inorganic metal NPs, several physicochemical parameters were optimized including pH, temperature, concentration of metal ion, extract volume and reaction time.

3.5.1.1 Effect of pH

pH was maintained at 5.0, 7.0, 8.0, 10.0, 12.0, and 14.0 by using 0.1 NaOH and HCl. The concentration of reaction mixture, the reaction time and temperature were kept constant. The absorbance of the solution was measured by the spectrophotometric approach to determine the optimum pH for the synthesis of ZnO nanoparticles.

3.5.1.2 Effect of Temperature

Temperature, was maintained at 25,30,33,36, 39, 41, 44, 47 and 50 ^{0}C, using a thermometer by keeping the concentrations of metal ions, the reaction time and pH of reaction mixture constant. The absorbance of the solution was measured by the spectrophotometric method.

3.5.1.3 Effect of Metal Ion Concentration

Concentration of metal ion was maintained at 0.01, 0.025, 0.046, 0.05 and 0.1M (0.01–0.1M). The concentration of seed extract, pH, temperature and incubation time of the solution were kept constant. The absorbance of the solution was measured at 300–800 nm as described above.

3.5.1.4 Effect of Reaction time

The reaction time effect was determined at room temperature at the interval of 0.5, 1, 2, and 4 h to study the effect of reaction time on the synthesis of NPs by keeping the pH, temperature and concentration of metal ion constant [35].

3.6 Analysis and characterization of ZnO nanoparticles

The synthesized plant mediated ZnO nanoparticles were analyzed using the following techniques. UV-Vis spectroscopy designed to detect the intense peak with in the wavelength range of 300-800 nm, to analyze electronic transition (Band gap) and the size, structure, stability, and aggregation of the synthesized zinc oxide nanoparticles. FTIR analysis was applied to identify the presence of functional groups in synthesized ZnO NPs and secondary metabolites in the plant extract. Hence, the dried powder of zinc oxide nanoparticles was grounded with KBr and cast into a pellet and made ready for analysis on the 65 FT-IR (Perkin Elmer) in range 4000-400 cm^{-1}spectrophotometer in the diffuse reflectance mode operating at a resolution of 4 cm^{-1}. A powder X-ray diffractometer (PXRD) (Rigaku miniflex600 XRD) (using K-alpha radiation of X-ray source a wavelength of 1.54059 Å, scan mode of 2theta/theta in 2θ range from 10-60°, to study crystalline particle size of ZnO NPs.

3.7 Photocatalytic degradation

Stock solution of methyl orange dye (5 X 10^{-5}M) was prepared in distilled water. It was further diluted as and when required. The photocatalytic degradation of MO dye was studied after addition of the catalyst 0.25 g of ZnO nanoparticles in 50 mL dye solution (0.05 mM). The whole setup was kept in dark and allowed ZnO to suspend in the MO solution for 30 min for physical adsorption equilibration. Initial concentration of MO, in term of light absorbance, was measured by UV-Vis spectrometer at 465 nm (wavelength range 200-600 nm). The whole solution was exposed to sunlight (30 -180 min). After a given irradiation time, about 2 mL of the mixture was withdrawn and the catalysts were separated from the suspensions by centrifugation (at 13000 rpm). The degraded solution was taken for absorbance measurement [36].

UV–vis absorption spectra (Aspect-1.2.3.6173, Analytic jena) and (UV-Jenway6705) monitoring the change in concentration of the organic dyes. The absorbance A_0 measured after stirring for 30 min in the dark was taken as the initial concentration C_0 of the solution. The absorbance A_t measured after variable periods of illumination was taken as corresponding to the residual concentration C_t. The degree of organic compound degradation was calculated by equation (1) [37].

Degradation efficiency (%) = C_0-C_t /C_0 *100= A_0-A_t/A_0 *100…… (1)

3.7.1 Optimization parameters photocatalytic degradation of methylene orange dye

3.7.1.1 Effect of photocatalysts dose

In order to examine the effect of photocatalyst dose on the bleaching and degradation of MO, different amount of catalyst from 0.05, 0.1, 0.15, 0.25 and 0.3 g (0.05 to 0.3 g) of ZnO nanoparticle were added to solution at a reaction time of 180 min, pH of 6 and initial MO concentration of 0.05 mM.

3.7.1.2 Effect of dye Concentration

In the photo catalysis process, one of the main parameters of discoloration of dye solution is dye concentration, so different concentration of dye, from 0.01, 0.025, 0.05, 0.075 and 0.1 mM (0.01-0.1 mM) of MO dye solution was removed at a reaction time of 180 min, pH of 6 and 0.3 g ZnO nanoparticle catalyst dose were kept constant.

3.7.1.3 Effect of pH

The pH-related experiments were carried out in the various pH values 4, 6,7,8 and 10 (4-10) with constant dose of 0.3 g of ZnO nanoparticle catalyst into 50 mL of the dye solution (0.025 mM) and reaction time of 180 min. The adjustment of the solution pH was conducted by 0.1 M HCl and 0.1 M NaOH solution [38].

3.8 Antibacterial Studies

The antibacterial activity was studied using the disk- diffusion method [34]. *Staphylococcus aureus, Escherichia coli, Bacillus subtilis* and *Klebsiella* were grown overnight on Mueller Hinton agar. A sterile cotton swab was dipped into the inoculum suspension and the swab was rotated several times with firm pressure on the inside wall of the tube to remove excess fluid. The swab was used to inoculate the dried surface of the Mueller Hinton agar by swabbing over the surface

of the agar, rotating the plate approximately by 90º to ensure an even distribution of the inoculum. Ciprofloxacin and dimethyl sulfoxide were used as positive and negative control respectively. An aqueous *Lepidium sativum* seed extract and ZnO nanoparticles were added on to the well of 6 mm diameter. The plates were incubated at 37 ºC for 24 h. Clear zones of inhibition around the wells were measured and calculated [34].

3.9 Methods of Data Analysis

Origin8.0 software was used to analyze the data collected from UV-Visible, XRD, and FT-IR spectroscopy.

4. RESULTS AND DISCUSSIONS

4.1 Physicochemical properties

In this study, the *Lepidium sativum* seed extract were tested for the presence of its phytochemicals, such as flavonoids, tannins, saponins, alkaloids and phenolics. The results of these qualitative phytochemical analysis of the *Lepidium sativum* extract are shown below in table 2.

Table 1: Lists of phytochemical groups and indications '+' shows presence'- 'absence

No	Phytochemicals	Test	Observation	Inferences
1	Flavonoids	2M sodium hydroxide	Yellow color	+
2	Tannins	5 % Ferric chloride	Yellow brown precipitates	+
3	Saponins	Distilled water	Froth	+
4	Alkaloids	Iodine and potassium iodide	Reddish-brown precipitate	+
5	Phenolics	1% Ferric chloride	Green color	+

The presence of phytochemicals in the seed extract was helped in the formation of ZnO nanoparticles by acting as both reducing and capping agent during ZnO NPs synthesis because of the presence of important functional groups like O-H, N-H, C=O, C=N and C=C within their structure.

For instance, the polyphenolic compounds such as flavonoids are very important plant constituents because of their electron donating ability via their –OH groups to act as reducing agent. The color changes in these tests are indicators for the formation of different complexes as a result of oxidation and reduction reactions in the phytochemicals presence testing process. For instance, the reddish-brown color for alkaloids indicates that the nitrogen or oxygen atoms of the amide groups of the alkaloids involve in a reaction. In most of the ferric chloride tests, the iron (III) ion forms complexes having different colors depending on the nature of the complexes. Moreover, the presence of phytochemicals conducted above in the crude extract as well as in the crystal lattice of the synthesized ZnO nanoparticles is responsible for their antimicrobial activities [39].

4.2 Synthesis of ZnO nanoparticles using Lepidium sativum seed extract

The color change in reaction mixture (metal ion solution and plant extracts) during the synthesis of nanoparticle were recorded through visual observation which was considered as an initial signature to formation of the target NPs [40]. When equal volume of 0.046 M of zinc acetate dehydrate react with seed extract the color of the mixture turned to pale white color up on the addition of 2M NaOH and stirring for 1 h it converted to yellow. These color changes might be due to the excitation of surface plasmon vibrations within the ZnO nanoparticles [41].

The appearance of yellow color precipitation in the reaction mixture indicates the formation of the respective nanoparticles. Particularly, flavonoids are believed to be responsible for conversion of Zn ions to ZnO NPs. The color changing in the solution was stopped further after a few hours, suggesting that the complete conversion of ZnO salt in to nanoparticle. These results have similar agreement with the previous reports [42].

4.2.1 Optimization of Physicochemical Parameters of ZnO NPs

The plant mediated synthesis of ZnO NPs by using *Lepidium sativum* seed extract was maintained in the absorption peak range of 300 - 800 nm. So, the sharp absorption peak was observed at 377 nm (Appendix 1(B)). In this study, the parameters for the synthesis of the target nanoparticles like pH, temperature, concentration of the metal ion and reaction time was optimized by measuring λ_{max} and considering the sharpest peak.

4.2.1.1 Effect of pH

At low pH (5), the formation of zinc oxide nanoparticles was not taking placed these might be due to repulsion occurred between positively charged H^+ and ZnO nanoparticles. The characteristics absorption peak of the ZnO NPs observed at 377 nm was found at pH of 10 (Appendix 2(c)). It suggested that the zinc acetate dihydrate was converted to ZnO NPs. While, at high pH 12- 14 the surface plasmon resonance (SPR) absorption peak shifted to larger wavelength (red shift) indicating the formation of larger size ZnO nanoparticles, broadening the observed peak.

Moreover, the strongly alkaline condition, the more abundance of OH^- ions in the solution form a complex with Zn^{2+} cations as the molecules Zn $[OH]_2^{4-}$ and Zn $(OH)_2$ which could restrain the production of ZnO nanoparticles. However, with increase in pH from 7 to 10, SPR absorption peak shifted to shorter wavelength (blue shift) confirmed to the formation of smaller size ZnO nanoparticles [44]. The spectra had single/sharp peak indicated that the synthesized nanoparticles

are specific. As a result of these pH 10 was found to be the optimum pH for the synthesis of zinc oxide nanoparticles (appendix 2(C)).

4.2.1.2 Effect of temperature

Increasing of the solution temperature lead to an increase in the size of the zinc oxide nanoparticles as a result no intense absorption peak and broadening of peak was observed from 33-50 ˚C (Appendix 3(C-J)). Therefore, this study has similar agreement with previous report [44]. While, at lower temperatures 25 and 30 ˚C the absorption peaks were obtained at 377 nm, but the better intense peak was observed at 25 ˚C (Appendix 3(A)) which suggested that the zinc acetate was converted into ZnO NPs and the synthesized nanoparticles are small in size, So RT was the optimum temperature needed for the synthesis of zinc oxide nanoparticles [35].

It has been demonstrated that, plant mediated synthesized ZnO nanoparticles size could be controlled by changing the solution temperature. The reduction rate of metal ions increased by temperature; because high temperature will lead to too high reaction kinetics. It is impossible to control the growth step of the crystallization process in reactions with fast kinetics [44].

4.2.1.3 Effect of Metal ion concentration

Synthesis of NPs was also affected by the concentration of zinc acetate dihydrates as the NPs formation was increased with increasing the concentration of zinc acetate dihydrates. While, at low concentration of 0.01 M no absorption peaks were observed, indicating that the dispersion of ZnO NPs was affected by the concentration [35].

When zinc ions concentration was increased biochemical reduction starts immediately. Further, the characteristic absorption peak at 377 nm was recorded in the concentration of 0.046 M. Thus, the narrow size distribution of ZnO nanoparticles and the optimum concentration of zinc acetate for ZnO nanoparticle via green route using *Lepidium sativum* extract was found to be 0.046 M [44] (Appendix 4(C)). The absorption spectra intensity of nanoparticles increased with increased concentration of precursor salt solutions [42].

4.2.1.4 Effect of reaction(incubation) time

Reaction time is also considered as an important factor for the synthesis of NPs, which also depends on the nature of metals. Reaction time is the period required for complete reduction of the

metal ions for the synthesis of metal NPs. The effect of incubation time was studied by keeping pH, temperature and concentration of zinc acetate dihydrate as constant [35].

As a result, after a time of 0.5 h no absorption peak was observed due to the instability of the synthesized ZnO NPs. The zinc oxide nanoparticles synthesized at optimum condition exhibited the sharpest peak obtained at 377 nm which was found to be stable after 4 h. (Appendix 5(D) [43].

4.3 Characterization of zinc oxide nanoparticles

4.3.1 UV-Vis Spectroscopy of the ZnO NPs

UV-vis spectroscopy which provides an information about the size and band gap energy of the nanoparticles. As a result, in the present study, the synthesized ZnO NPs was confirmed by the absorption maxima at the wavelength of 376 nm. The occurrence of these absorption peak is due to surface plasmon resonance property of the nanoparticle which occurs owing to oscillation of free electrons on the surface of the nanoparticle when they align in resonance with wavelength of irradiated light [44]. The obtained peak was even sharper and more intense it is expected to be the effect of smaller size of the as synthesized ZnO nanoparticles [39]. No other peaks were observed in the spectrum, which confirms that the synthesized product is only ZnO nanoparticles [47].

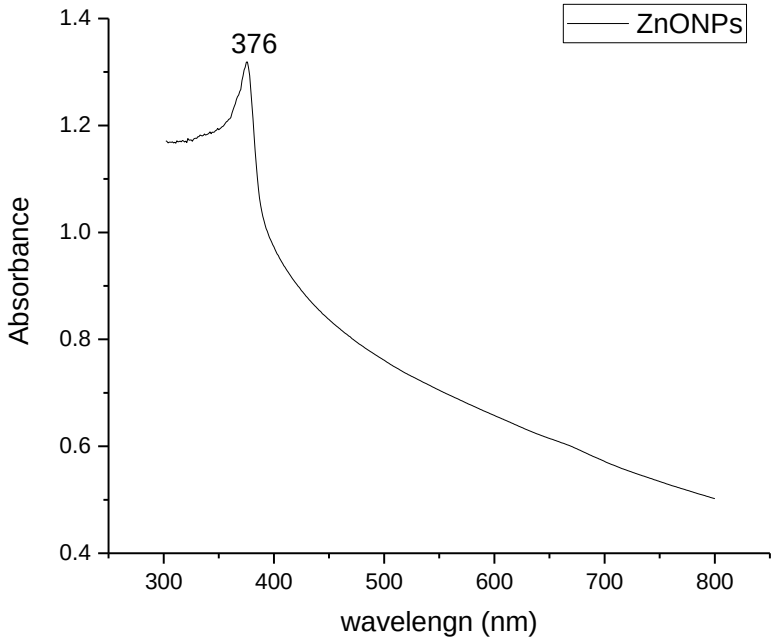

Figure 5. UV-Vis spectrum of synthesized ZnO NPs (λ_{max}=376 nm)

The spectrum reveals the characteristic absorption peak at 376 nm (figure (5) shows the synthesized ZnO NPs exhibited a bandgap value of 3.08 eV (Figure 6), which can be assigned to the intrinsic band-gap absorption of ZnO [46]. As particle size decreases band gap increases as a result of quantum size effect on electric energy bands of semiconductor [47].

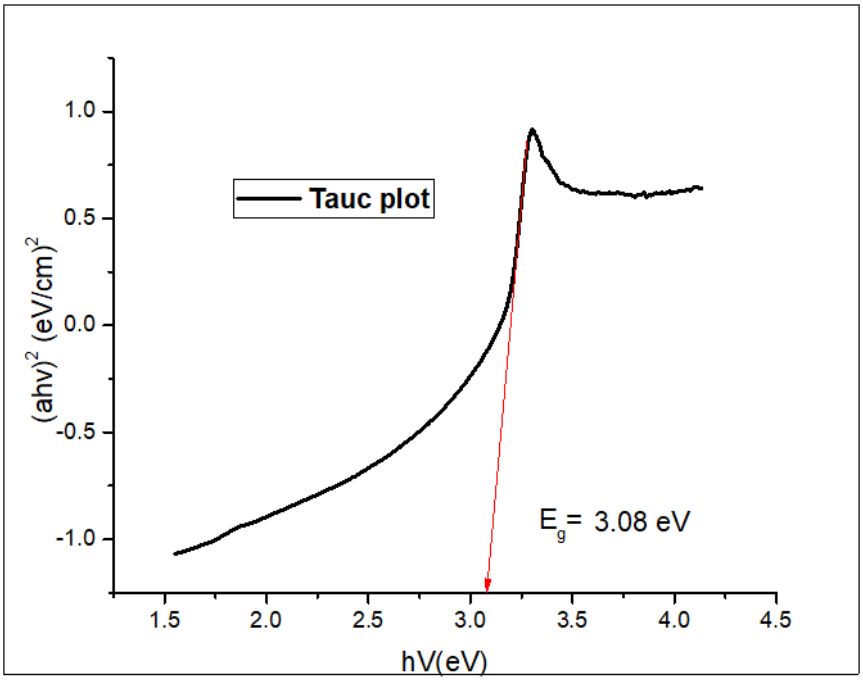

Figure 6. Plot of $(\alpha h\nu)^2$ vs hν, band gap energy of the synthesized ZnO NPs.

Band gap energy was given by Tauc relationship (P. Bindu and S. Thomas.2017). In equation (2)

$$(\alpha h\nu)^2 = K\,(h\nu - E_g) \quad \ldots\ldots\ldots\ldots\ldots\ldots\ldots\ldots \quad (2)$$

Where, α is absorption coefficient was calculated from absorbance A and the sample thickness t. h is plank's constant ($6.62.10^{-34}$ Js^{-1}), K is constant (2.3026) and E_g is band gap energy. Therefore, the estimated band gap value of the synthesized ZnO nanoparticle was found to be 3.08 eV as shown above (figure 6).

The UV-vis spectrum of the synthesized zinc oxide nanoparticles is shifted to longer wavelength as compared to the plant extract. This shows that during the formation of the nanoparticles, there is a red shift in wavelength which can be considered as an indicator of a newly formed particles with different surface plasmon resonance [39].

The UV-Vis spectrum of plant extract (Figure 7) is characterized by absorptions in the UV region (220-280 nm) and in the range 330-420 nm, corresponding to phenolic acids and their derivatives (flavones, flavanols, phenylpropenes and quinones). The *Lepidium sativum* seed extract have similar fingerprints, being the richest in phenolic derivatives (272 nm) and flavonoids (around 322 nm) [48].

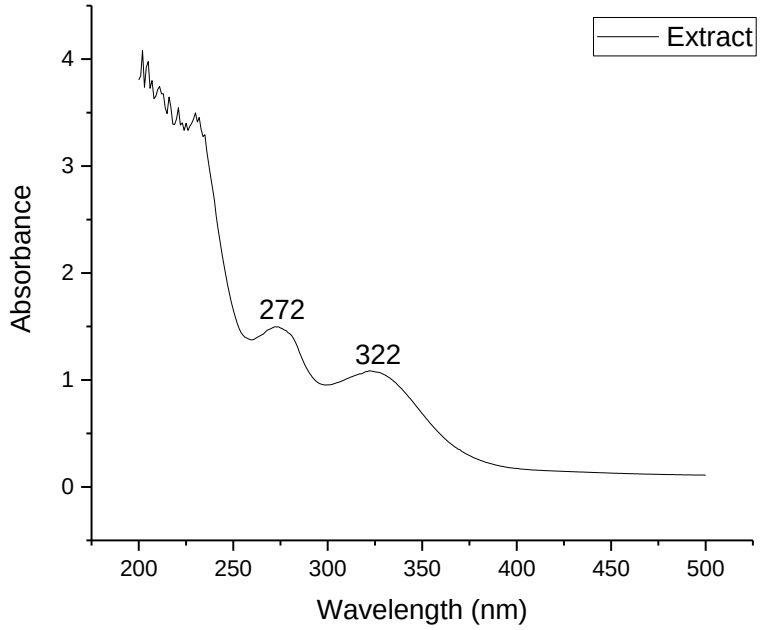

Figure7. UV-vis spectrum of *Lepidium sativum* seed extract.

4.3.2 FTIR Spectroscopy of the ZnO NPs

The FTIR spectra were used to confirm the presence of functional group and plant metabolites which are used in the reduction, capping and stabilization of the green synthesized zinc oxide nanoparticles. The FTIR spectra of the synthesized zinc oxide nanoparticles Figure 8(a) depicts, a broad band absorption peak at 3390 cm^{-1} indicates the stretching of O–H groups in water, alcohol and phenols. Peaks at 2923 and 2853 represent that the plane bending of C-H and C-C bonds of the alkyl groups [34]. The peak at 1077 and 1007 cm^{-1} are ascribed to C-O bond stretching vibration of biomolecules from seed extract. The peaks at 1518 cm^{-1} are assigned to C=C stretch of alkenes. The peaks at 1569 cm-^{1} implies to C=O stretch of amides. Peaks at 1402 cm^{-1} C-N

stretching of amine groups. The major absorption band at 559 and 443 cm^{-1} are characteristic to the Zn-O bond [49].

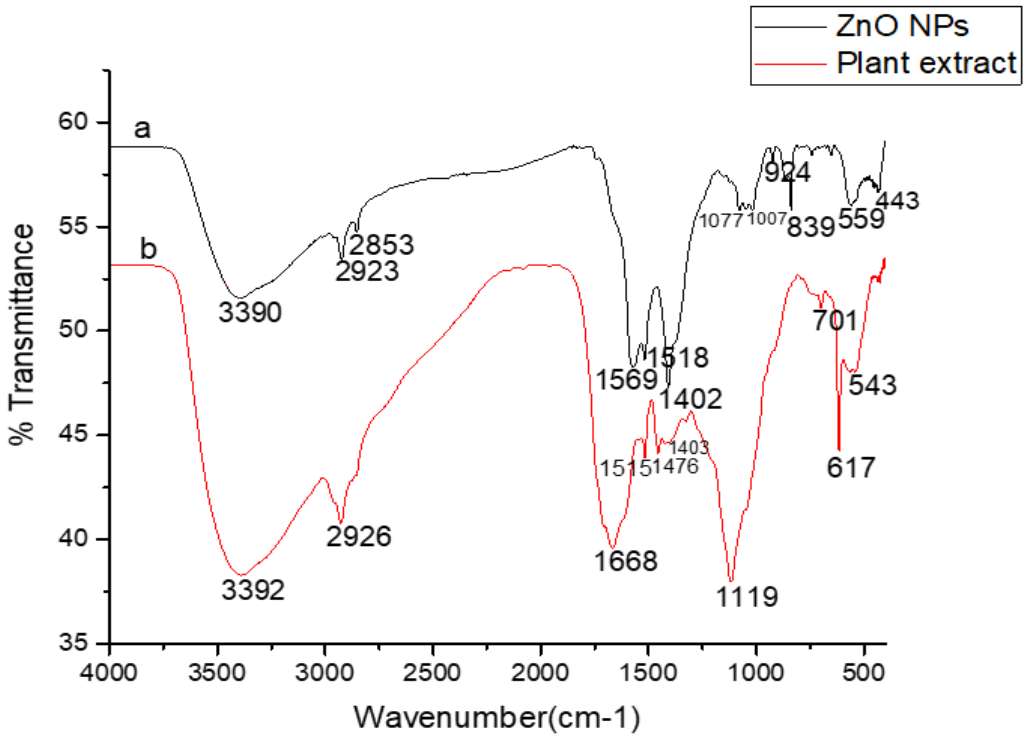

Figure 8. **(a)** FT-IR spectra for ZnO NPs **b)** FT-IR spectra for seed extract of *Lepidium sativum.*

FTIR spectra of the biosynthesized ZnO NPs showed a small shift with slight changes to lower wavenumber (red shift) in some related peaks and in their intensities, functional groups like OH, C=O and C-N suggesting that the major biomolecules from the extract were capped or bonded to the surface of ZnO NPs.

FTIR spectra of *Lepidium sativum* seed extrac as shown in Figure 8(b) represent, broad and inten se absorption peak at 3392 cm^{-1} might be due to overlapped OH and NH stretching. The other peaks at 2926 cm^{-1} (C-H) stretching, 1668 cm^{-1} (C=O) of phytochemicals, 1403 cm^{-1} (C-N) of amine, 1392 cm^{-1} (C-H) of the alkene group, 1515 cm^{-1} (N-H) stretch, 1476 cm^{-1} (C-H) bending and 1119 cm^{-1} (C-O) stretch [50]. Further, peaks at 701,617 and 543 cm^{-1} (RCOO) of phytoconstituents, which are rich in polyphenols, carboxylic acid, polysaccharide, amino acid and proteins, which are involved in the reduction and stabilization (capping) of ZnO NPs. Our results are consistent with the previous study report [34].

4.3.3 XRD studies of ZnO-NPs

The crystalline nature of the zinc oxide nanoparticles synthesized from *Lepidium sativum* seed has been studied by XRD analysis. The XRD diffractogram clearly shows the main peaks at (2θ) range from 10º to 60º (Figure 9). The XRD spectrum of the zinc oxide nanoparticles showed five most diffraction peaks at, 32.8, 34.72, 36.56, 47.84 and 56.88° corresponding to the (hkl) values of (011), (110), (111), (021) and (202) planes respectively. So, it was confirmed that the synthesized zinc oxide nanoparticles are crystalline and hexagonal wurtzite structure which is the most stable phase of ZnO.

The broadening of the peaks in XRD indicates the formation of nanosized particles. The XRD peaks are broader as the NPs size decreases. Our result has similar agreement with the previous report [40]. There were unallocated peaks that appeared at 29.68, 33, 43.06 and 53.06°, these unpredicted crystalline structures could be due to impurities raised from the precursor (zinc acetate dihydrate) salts a result crystallization is occurred on the surface of the zinc oxide nanoparticles.

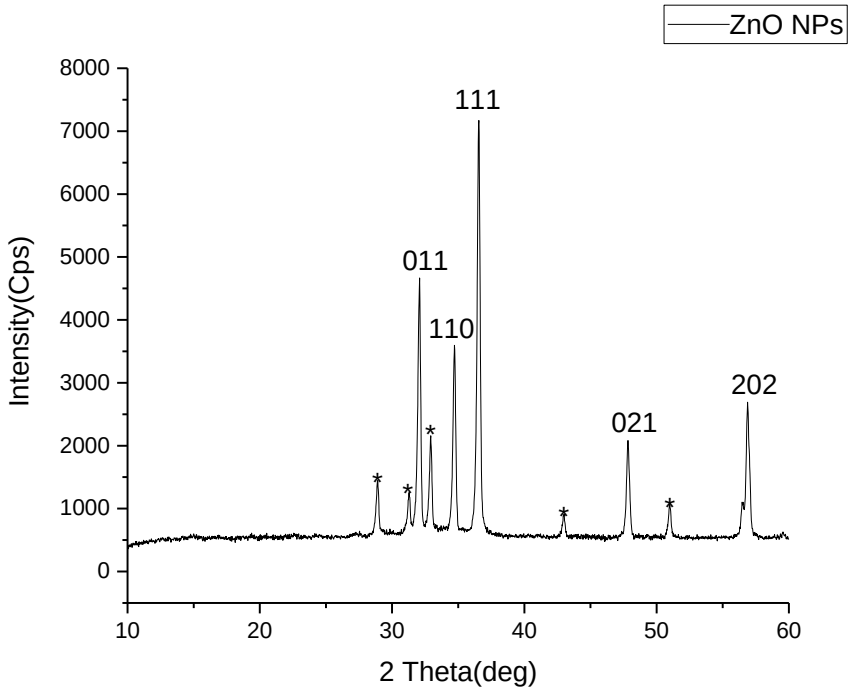

Figure.9 PXRD of Zinc oxide nanoparticles showing five peaks are given 2θ values.

The crystallite size of ZnO NPs was calculated from the most intense peaks using Debye–Scherrer's formula, by equation (3)

$$D=K\lambda/\beta \cos\theta \quad \ldots\ldots\ldots\ldots\ldots\ldots\ldots\ldots\ldots\ldots \quad (3)$$

Where D is crystallite particle size, K is Scherrer's constant (0.9), λ is the wavelength of X-ray (1.54059 Å =0.154059 nm), β is the full width at half maximum (FWHM) of the intensity peaks, and θ is the Bragg's diffraction angle. The most intense peak was observed $2\theta=36.56$, at hkl (101). While $\theta=18.28$,18.28/180=0.1015 = 0.995

$$\beta = 0.2748 = 0.2748*3.14/180=0.0048$$

$$D=0.9*0.154059 \text{ nm} / (0.0048) *(0.995)$$

$$= 0.13865 \text{ nm} /0.00477$$

$$= \underline{\mathbf{29 \text{ nm}}}$$

As a result, the calculated value of the synthesized zinc oxide nanoparticle has crystalline size of 29 nm.

4.4 Photocatalytic degradation

In the present study, the photocatalytic degradation of methyl orange (MO) dye was studied by the synthesized zinc oxide nanoparticles using *Lepidium sativum* seed extract via solar irradiation technique in 30 min time interval (30, 60, 90, 120, 150 and 180 min) dye degradation which was visually detected by a gradual change in the color of dye solution from orange to colorless (appendix 6(A) and the characteristic absorption peak of MO was found to be 464 nm.

However, the colour could not be completely degraded to water after completing the final reaction time at 180 min this might be due to dissolution occur between the dye molecule and ZnO NPs [52]. Further, this might be due to charge separation between electron and hole pairs in the excited states that prevents recombination of charge pairs for a longer time under visible radiation [53].

4.4.1 Optimization of photocatalytic degradation of MO dye

4.4.1.1 Effect of catalyst dose

It was observed that increasing catalyst dose from 0.05 to 0.3 g in a reaction time of 180 min which leads to an increase in the percentage of MO degradation 57.5 to 82 % respectively. The results showed that, the removal efficiency of MO increased with respect to the time of irradiation and the quantity of ZnO nanoparticles (Figure 10). Here, with the increase in the dose of the nanoparticles the rate of removal is rapidly increasing due to enhancement of active sites which increases in the number of hydroxyl radicals and superoxide [5]. Besides, it could be due to the mount of electron-hole pairs was formed during the UV light irradiation [37]. Therefore, catalyst dose of 0.3 g was found to be optimum and selected for further studies.

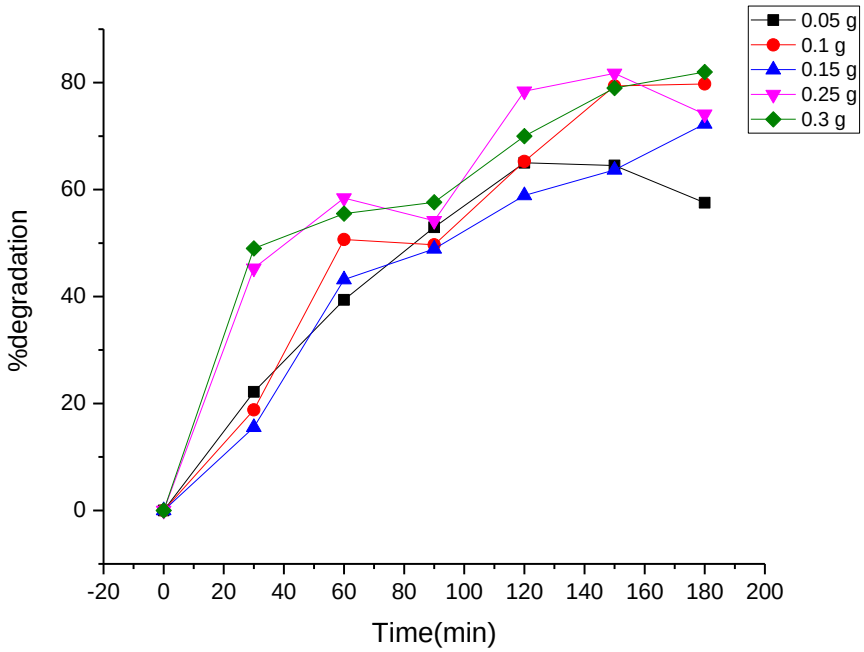

Figure 10. The effect of catalyst amount on the dye degradation of MO. Methyl orange of 0.05 mM, pH 6 and time 180 min

However, excessive use of catalyst quantity which forms milky solution leads to preventing penetration of UV light onto the catalyst surface which could decrease production of hydroxyl radicals as a result which decreases efficiency dye damage and discoloration of solution [38].

4.4.1.2 Effect of dye concentration

The degradation of MO dye is also affected by the concentration of MO dye. Varying dye concentration (0.01-0.1 mM) with constant dose of ZnO catalyst 0.3 g, reaction time 180 min and initial pH of 6. The relative degradation (99.1%) was obtained by using 0.025 mM concentration. The efficiency of methyl orange dye removal was gradually increase with time in 0.025 mM concentration of dye (Figure 11). Therefore, 0.025 mM of dye was the optimum concentration used for further studies [38].

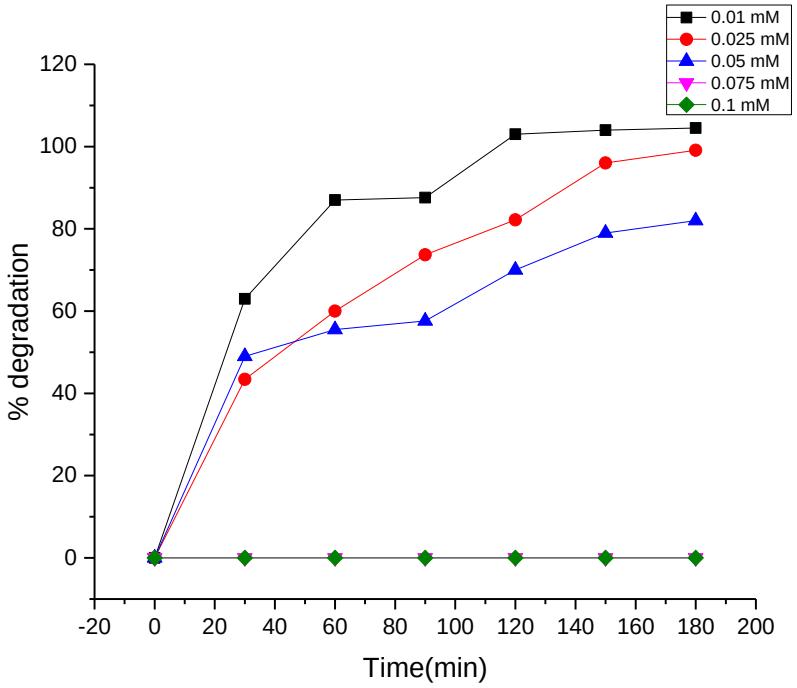

Figure.11 The effect of dye concentration on the degradation of MO. Catalyst dose of ZnO NPs 0.3 g, pH 6 and time 180 min

However, at higher dye concentration (0.075 mM and 0.1 mM) the exposure of the radiation photons to the catalyst surface is hindered and screened off thereby reducing the photocatalytic activity in the system. Moreover, the number of collisions between dye molecules increases at the

cost of required collisions between dye molecules and $OH^{\cdot}$ radical and therefore, the rate of degradation is retarded [54].

4.4.1.3 Effect of pH

The effect of pH was studied by talking the optimum amount of catalyst dose 0.3 g, dye concentration 0.025 mM and reaction time 180 min. While, varying pH of the solution in the range of 4-10. The pH of solutions greatly affects the rate of reaction taking place on semiconductor surfaces due to its influences on surface-charge-properties of the photocatalysts. The highest efficiency of photodegradation was observed at pH of 6 with 99 % efficiency (Figure 12). Methyl orange is an anionic dye; therefore, it is expected that more dyes absorbed at lower pH where ZnO surface is positively charged [55]. So, pH 6 was optimum pH selected for further studies.

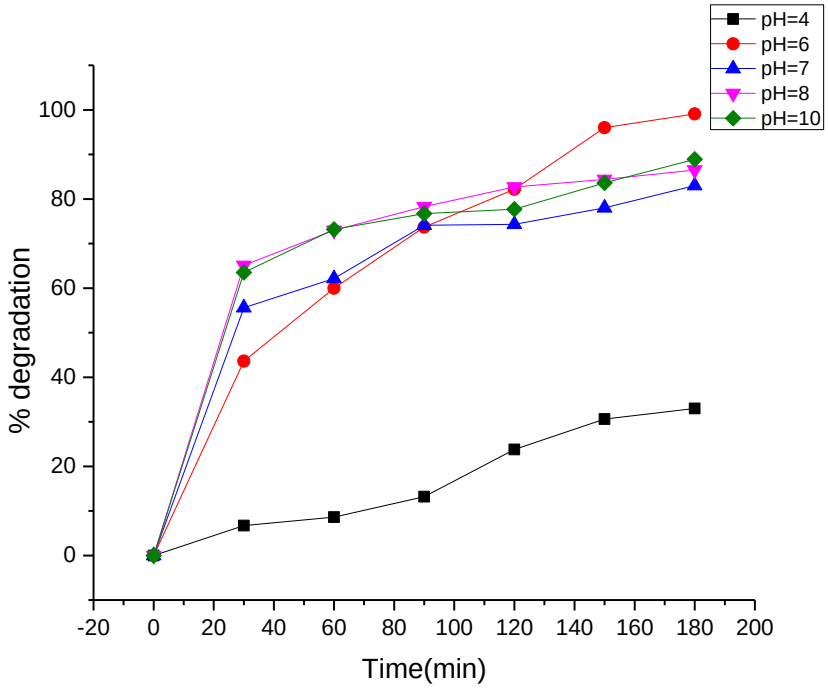

Figure 12. The effect of pH on the degradation of MO with 0.025 mM dye concentration, Catalyst dose ZnO of 0.3 g and time 180 min.

At a lower pH (pH=4) the photocatalytic degradation is lower might be due to the less availability of OH^{-} ions to form highly active $OH^{\cdot}$ radicals. At higher pH (pH,8-10) sorption of negatively charged MO on the similarly charged photocatalyst decreases due to ion-ion repulsion and hence

there is less photocatalytic degradation of MO dye [55]. Moreover, because of this fact that the oxidation potential of hydroxyl radical decreases with increasing pH of the solution [56].

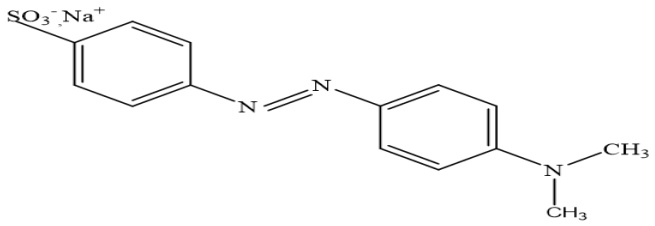

Structure of MO dye

After optimization, the optimized methyl orange dyes having catalyst dose of ZnO NPs of 0.3 g concentration of MO dye 0.025 mM and PH 6 were taken. Then after, the photocatalytic degradation of MO dyes was taken place in the presence and absence of ZnO nanoparticle catalyst as a function of time with maximum wavelength 464 nm.

Degradation of methyl orange were visualized by the decrease in the peak intensity with in 180 min. The adsorption ZnO NPs on to the methyl orange solution was initially low and further increase with constant increase of time [52]. As shown figure 13(B), the decolorization rate is very low and does not occur complete degradation or mineralization and also there is no considerable shift in peak position without exposure of ZnO photocatalyst. Whereas, figure 13(A), an effective bleaching and degradation was occurred and the gradual decrease in peak intensity was found in the presence of ZnO nanoparticle catalyst. Generally, this indicates that an effective bleaching rate and degradation of methyl orange occur due to photochemical reaction in the presence of ZnO catalyst in time 180 min as compared to in the absence of photocatalyst degradation and bleaching processes were almost negligible. The present result is in agreement with the previous report [38].

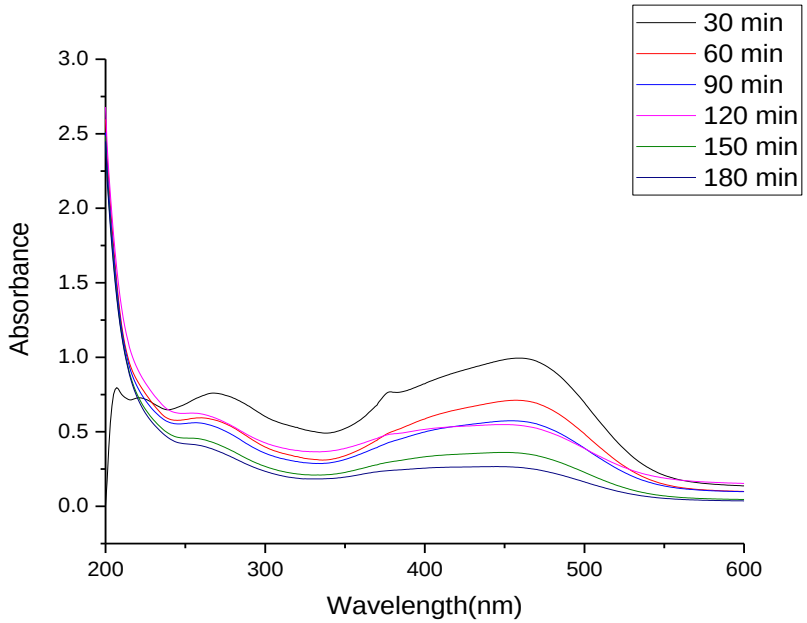

Figure13 (**A**). Time dependent absorption spectra of Methylene orange dye in the presence of ZnO NPs 0.3 g photocatalyst, methyl orange 0.025 mM and pH 6.

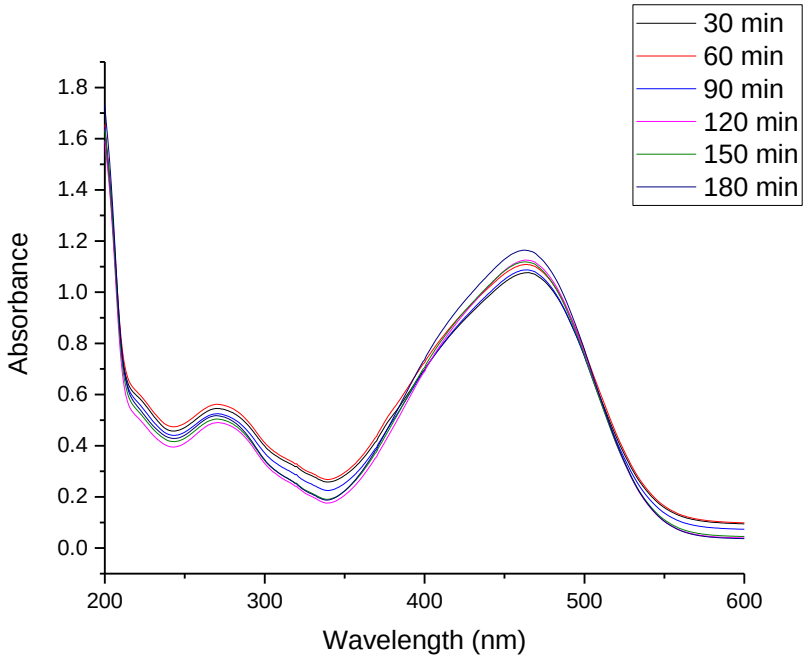

(B). Time dependent absorption spectra of Methylene orange dye in the absence of ZnO NPs photocatalyst, methyl orange 0.025 mM and pH 6.

4.5 Antimicrobial activity study of ZnO NPs

The antibacterial activity of the synthesized ZnO NPs using *Lepidium sativum* seed extract and the pure *Lepidium sativum* seed extract was investigated on *Klebsiella, Escherichia coli, Staphyloco ccus aureus,* and *Bacillus subtills* bacteria (figure (14) or (Appendix 7(A-D)). *Lepidium sativum* plant seed extract contains a number of carbonyls, carboxyl, and hydroxyl groups in polyphenols. and the presence of abundant hydroxyl and carbonyl groups is responsible for antibacterial applications. The existence of these compounds in the extract and the surface helps ZnO NPs to adhere to the bacterial cell membranes. The chemical interaction between the extract molecules and ZnO NPs enhance the reactivity of NPs and improves penetration via bonding to the surface of the bacteria.

.

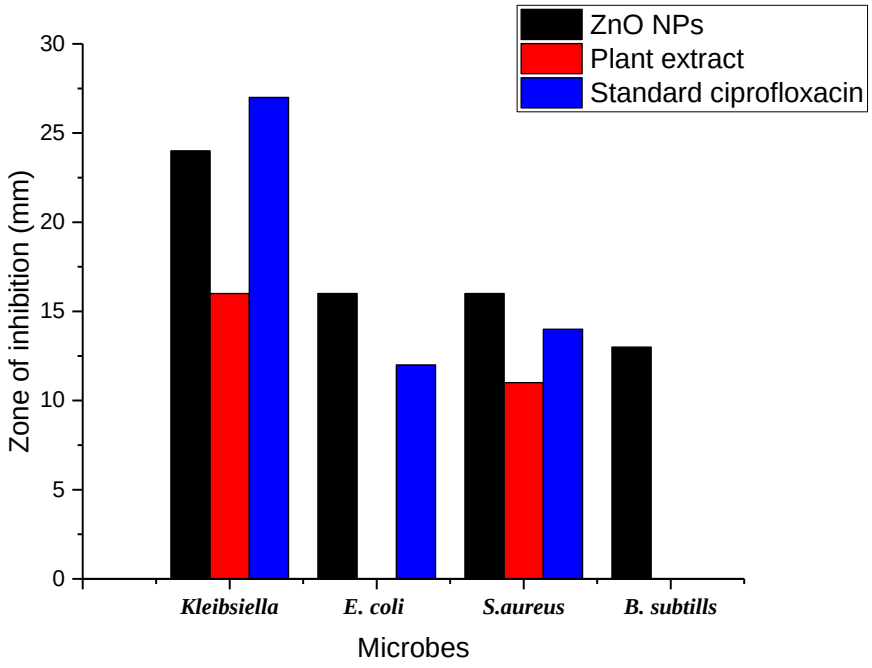

Figure 14. Antibacterial activity of the biosynthesized ZnO NPs, *Lepidium sativum* extract and ciprofloxacin against *B. subtills*, *S. aureus*, *Klebsiella* and *E. coli*

The synthesized zinc oxide nanoparticles are more susceptible against gram negative bacteria than gram positive bacteria as the opposite charge enhances the interaction between the bacteria layer and the ZnO NPs. Moreover, gram-positive bacteria have a triple thin layer of peptidoglycan compared with Gram-negative bacteria and show more toleration to nanoparticle interaction with the cell membrane. Besides, the good antibacterial activity could be due to the smaller sized of the nanoparticles can easily penetrate to the cell of the bacteria. The entry of ZnO NPs into the cell leads to integrity loss of phospholipid layer and blebbing of intracellular elements resulting in cell death. Furthermore, the green synthesized nanoparticles show more antibacterial activity than that of the plant extracts [51].

Table 2: Summary of antibacterial activity assay

Zone of inhibition in diameter(mm)			Negative control	Positive control(mm)
Bacterial strain	ZnO NPs 100 mg/mL	*Lepidium sativum* extract (100 mg/mL)	DMSO	Ciprofloxacin (20µg)
Escherichia coli	16 mm	-	-	12 mm
Bacillus subtills	13 mm	-	-	-
Staphylococcus aureus	15 mm	11 mm	-	14 mm
Klebsiella	24 mm	16 mm	-	27 mm

Based on the above data, the antibacterial activity of zinc oxide nanoparticle against gram negative bacteria, *klebsiellas* has greater activity than plant extract. Regarding Gram positive bacteria, the zinc oxide nanoparticles show better activity to against *Staphylococcus aureus* than the plant extract. The zinc oxide nanoparticle has a potential to against all four bacterial strain than the plant extract. The synthesized zinc oxide nanoparticle has greater activity to against gram-negative bacteria *(Escherichia coli* and *Klebsiella)* than the gram-positive bacteria *(Staphylococcus aureus* and *Bacillus subtills).*

Moreover, the synthesized ZnO NPs exhibited a considerable zone of inhibition for *Escherichia coli* and *Klebsiella* compared with *Staphylococcus aureus* and *Bacillus subtills*. The observed zones of inhibitions with 100 mg/mL concentration of ZnO NPs were 24, 16, 15 and 13 mm for *Klebsiella, Escherichia coli, Staphylococcus aureus,* and *Bacillus subtills* respectively.

5. CONCLUSION AND RECOMMENDATIONS

5.1 Conclusion

A green method for the synthesis of zinc oxide nanoparticles using seed extracts of *Lepidium sativum* has been demonstrated. The metal oxide nanoparticles were characterized by UV-Vis, FT-IR and XRD. The Synthesized of zinc oxide nanoparticles was optimized based on parameters like pH, temperature, metal ion concentration and reaction time to demonstrate the maximum wavelength of intense peak. The FT-IR spectroscopy revealed different secondary phytochemicals like flavonoids, alkaloids, and others were around the synthesized zinc oxide nanoparticles. The XRD result revealed the crystalline nature of the synthesized zinc oxide nanoparticles. The photocatalytic degradation of MO dye was optimized by parameters such as catalyst dose, dye concentration and pH. Degradation of MO dye by ZnO catalyst was efficient for bleaching of dyes due large band gap energy and small size. The degradation of MO dye in the presence of ZnO catalyst was efficient as compared to in the absence of catalyst. The synthesized zinc oxide nanoparticles have been exhibited significant antibacterial activity against all the four bacterial strains. These are the gram positives bacterial *Staphylococcus aureus* and *Bacillus subtills*, the gram negatives bacterial *Escherichia coli* and *Klebsiella*. The synthesized zinc oxide nanoparticles have greater antibacterial activity to against gram negative bacteria than gram positive bacteria. The synthesized zinc oxide nanoparticles have greater antibacterial activities than the seed extracts of *Lepidium sativum.* Generall*y,* Plant mediated synthesis of metal oxide nanoparticles have an application for photocatalytic degradation of MO dye and as antibacterial agent against human pathogenic diseases.

5.2 Recommendation

For further work, it was recommended that additional characterization for further size determination and morphology of the sample using instruments; SEM, TEM and EDX. The application of ZnO NPs as degrading dyes needs further work. Further work is also required on other metal oxide nanoparticles through mediation of *Lepidium sativum* seed extract with application of their antimicrobial agents and photocatalytic activity. Commonly peoples have been using seed as antimicrobial agent against pathogens, but using in excess amount have side effect which induce abortion. Therefore, care is needed to use the seed alone. Traditionally peoples have

been using the seed as antimalarial agent to reduce fever disease but, this strictly needs further investigation.

6. REFERENCES

1. Ansari, M.O.; Khan M.M.; Ansari S.A.; Cho M.H. Polythiophene nanocomposites for photodegradation applications: Past, present and future. *J. Saudi Chem. Soc*.**2015**, *19*, 494-504.
2. Kumar, M.; Sivakumar V.; Tamilarasan, R. Adsorption of Victoria blue by carbon/Ba/A lignate beads: kinetics, thermodynamics and isotherm studies. *Carbohydrate. Polym*.**2013**, *98*, 505-513.
3. Jamal, N.; Radhakrishnan, A.; Raghavan. R.; Bhaskaran. B.; Access, O. Efficient photocatalytic degradation of organic dye from aqueous solutions over zinc oxide incorporated nanocellulose under visible light irradiation. **2020**:84-91.
4. Bazrafshan, E.; Zazouli, M. A. Adsorptive removal of methyl orange and reactive red dyes by *Moringa Peregrina* Ash. **2014.**
5. Pirsaheb, M.; Hossaini. H.; Nasseri, S.; Azizi, N.; Shahmorad, B.; Khosravi, T. Optimization of photocatalytic degradation of methyl orange using immobilized scoria - Ni / TiO nanoparticles. *J Nanostructure Chem*. **2020**.
6. Hussain, I.; Singh, N. B.; Singh, A.; Singh, H.; Singh, S. C. Green Synthesis of nanoparticles and its potential application. *Biotechnol. Lett*. **2016**, *38*, 545-560.
7. Kadam, P. V.; Yadav, K.; Shivatare, R. *Lepidium sativum* Linn: *an ethnobotany*. 2012,
8. Khaldakar, M.; Butala, D. The Synthesis and Characterization of metal Oxide nanoparticles and its application for photo catalysis. **2017**, *7*, 499–504.
9. Oudhia.A.; Sharma, S. Study of photocatalytic degradation of methyl orange by ZnO catalysts synthesized through biotemplates.**2016**.
10. Yu, X; Wu, Y. Facile synthesis of ZnO nanoparticles for the photocatalytic degradation of methylene blue.**2017**.
11. Thema, F.T.; Manikandan. E.; Dhlamini, MS.; Maaza. M. Green synthesis of ZnO nanoparticles via *Agathosma betulina* natural extract. *Materials Letters*. **2015**,*161*,124-127.
12. Khandel, P.; Kumar, R.; Deepak, Y.; Soni, K.; Kanwar, L.; Kumar, S.; Silver, A. Biogenesis of metal nanoparticles and their pharmacological applications: Present status and application Prospects; *Springer Berlin Heidelberg*, **2018**; *8*.

13. Besufekad, Y.; Beri, S.; Adugnaw, T.; Beyene, K. Antibacterial Activity of Ethiopian *Lepidium Sativum* L. against Pathogenic Bacteria. **2018**, *12*, 64–68.
14. Wadhwa, S.; Agrawal, A.; Saini, N.; Patidar, L. N. Pharmacognostical study of *Lepidium sativum*.**2012,** *2*, 316–323.
15. Shah, M.; Fawcett, D.; Sharma, S.; Tripathy, S. K. Green Synthesis of metallic nanoparticles via biological entities; **2015**, *8*, 7278–7308.
16. Reverberi, A. P.; Vocciante, M.; Lunghi, E.; Pietrelli, L. New trends in the synthesis of nanoparticles by green Methods. **2017**.
17. Singh, J.; Dutta, T.; Kim, K. H.; Rawat, M.; Samddar, P.; Kumar, P. Green Synthesis of metals and their oxide nanoparticles: applications for environmental remediation. *J. Nanobiotechnology* **2018**,1–24.
18. García, R.; Pedraza, J. Protective effect of curcumin against heavy metals induced liver damage. *Food and chemical toxicology*. **2014**, *69*, 182-201.
19. Abdelghany, A. M.; Meikhail, M. S.; Abdelraheem, G. E. A.; Badr, S. I.; Elsheshtawy, N. *Lepidium sativum* natural seed plant extract in the structural and physical characteristics of polyvinyl alcohol. *Int. J. Environ. Stud.* **2018**, 1–13.
20. Marslin, M.; Siram, G.; Id, K.; Q. K.; Selvakesavan, R. K.; Kruszka, D.; Kachlicki, P.; Franklin, G. Secondary metabolites in the green synthesis.**2016**,1-3.
21. Anulika, N. P.; Ignatius, E. O.; Raymond, E. S.; Osasere, O.; Hilda, A. The chemistry of natural Product: Plant secondary metabolites. **2016**.
22. Herawati. N.; Suzuki, S.; Hayashi, K.; Rivai, IF.; Koyoma, H. Cadmium, copper and zinc levels in rice and soil of Japan, Indonesia and China by soil type. *Environmental contamination and toxicology*. **2000**, *64*, 33-39.
23. Parveen, K.; Banse, V.; Ledwani, L. Green Synthesis of nanoparticles: their advantages and disadvantages. **2016**.
24. Lu, H. N.; Güngör, A. A.; Nce, S. İ. Synthesis of nanoparticles by green synthesis method. **2017**, 2–6.
25. Patra, J. K.; Baek, K. Factors affecting synthesis and characterization techniques. *Green Nanobiotechnology*: **2014**.
26. Kanagasubbulakshmi, S.; and Kadirvelu. K. Green Synthesis of iron Oxide nanoparticles using *Lagenaria siceraria* and evaluation of its antimicrobial activity. **2017**.

27. Mourdikoudis, S.; Pallares, R. M. Characterization techniques for nanoparticles: comparison and complementarity upon studying. **2018**, 12871–12934.
28. Nava, OJ.; Luque, P.; Gomez Gutierrez, CM.; Vilchis-Nestor, AR.ML. Influence of *Camellia sinensis* extract on zinc oxide nanoparticle green synthesis. *Journal of Molecular Structure*. **2017**, *1134*, 121-125.
29. Chowdhury, H. I; Hossain, M. S; Azad, M. Z; Islam, and Dewan, M. A. Photocatalytic degradation of methyl orange under UV using ZnO as catalyst.”.**2018**,*06*.
30. Cowan, MM. Plant products as antimicrobial agents. **1999**; *12*, 564.
31. Taran, M.; Rad, M.; Alavi, M. Biosynthesis of TiO and ZnO nanoparticles by halomonas elongata IBRC-M 10214 in different conditions of medium. *BioImpacts: BI.* **2018**, *8*, 81-89.
32. Ghalem, BR.; Ali, B. Preliminary phytochemical screening of five commercial essential oils. **2017**, *2*, 145-151.
33. Veeramanikandan, V.; Madhu, G. C.; Pavithra, V.; Jaianand, K.; Balaji, P. Green synthesis, characterization of iron oxide nanoparticles using *Leucas aspera* leaf extract and evaluation of antibacterial and antioxidant Studies. **2017**, *6*.
34. College, sm.; College, sm. Green synthesis and its applications of magnesium oxide nanoparticles from the seeds of *Lepidium sativum*. **2016**, *7*, 14029-14032.
35. Gupta, M.; Tomar, RS.; Kaushik S, Mishra RK. Effective antimicrobial activity of green ZnO nanoparticles of *Catharanthus roseus*. **2018**, 91-13.
36. Chowdhury, MIH.; Hossain, MS.; Azad, MAS.; Islam, MZ.; Dewan, MA. Photocatalytic degradation of methyl orange under UV using ZnO as catalyst. **2018**.
37. Abbasi S. Photocatalytic degradation of methyl orange by ZnO and SnO2 nanoparticles. **2015**.
38. Sadat, M.; Mojtaba, N.; Seyedeh, H.; Ghasemi, S.; Arab, M. Synthesis of ZnO nanostructure using activated carbon for photocatalytic degradation of methyl orange from aqueous solutions. *Appl. Water Sci*. **2018**.
39. Kelele, K. G.; Kahsay, M. H. Green Synthesis of CuO nanoparticles using leaf extract of *Catha edulis* and its antibacterial activity. **2019**.

40. Shekhawat, M.; MS. Green synthesis of zinc oxide nanoparticles using plant extracts of *Leucas aspera* (willd) L. *Journal of Biological Papers* **2016**,22-27.
41. Gopalakrishnan, Y.; Tun, U.; Onn, H. Green synthesis of ZnO nanoparticles by *Coriandrum sativum* leaf extract: *structural and optical properties*. **2019**.
42. Saranya. S.; Eswari, A.; Gayathri, E.; Eswari. S.; Vijayarani K. Green Synthesis of metallic nanoparticles using aqueous plant extract and their antibacterial activity. **2017**.
43. Jamdagni, P.; Khatri, P.; Rana, JS. Green synthesis of zinc oxide nanoparticles using flower extract of *Nyctanthes arbor-tristi*s and their antifungal activity. *J King Saud Univ - Sci*. **2018**, *30*,168-175.
44. Nadernejad, N.; Hashemi, S. Green synthesis of ZnO nanoparticles by Olive (*Olea europaea*). **2017.**
45. Umavathi, S.; Ramya. M.; Padmapriya. C.; Gopinath K. Green Synthesis of zinc oxide nanoparticle using *Justicia procumbense* leaf extract and their application as an antimicrobial agent. **2020**, 1866.
46. Awad, MA.; Aldosari, NS.; Alghannam, SF. Greener synthesis of zinc oxide nanoparticles: characterization and multifaceted applications. **2020**,1-14.
47. Estrada, J.; Cruz, A.; Santander, M.; Abraham, M.; Alma, V. Nanoscale zinc oxide particles for improving the physiological and sanitary quality of a mexican landrace of red maize. **1999**,1-12.
48. Medicine, V.; Science, CF.; Bunghez, F.; Socaciu, C.; Pop, R.; Ranga, F. Characterization of an aromatic plant-based formula using UV-Vis Spectroscopy, LC-ESI (+) QTOF-MS and HPLCDAD analysis. **2013**.
49. Abdelkhalek, A.; Alaskar, A. Green synthesized ZnO nanoparticles mediated by *Mentha spicata* extract induce plant systemic resistance against tobacco mosaic virus. *J of Applied Sciences*.**2020**.
50. Ashokkumar, R.; Ramaswamy, M. Phytochemical screening by FTIR Spectroscopic analysis of leaf extracts of selected indian medicinal plants. *Original research article*. **2014**, *3*, 395–406.
51. Alamdari, S.; Ghamsari, M. S.; Lee, C.; Han, W.; Park, H.; Tafreshi, M. J.; Afarideh, H. Preparation and characterization of zinc oxide nanoparticles using leaf extract of *Sambucus ebulus*. *Applied Sciences*.**2020**, 1–19.

52. Kumar, P.; Govindaraju, M.; Senthamilselvi, S.; Premkumar, K. Biointerfaces photocata lytic degradation of methyl orange dye using silver (Ag) nanoparticles synthesized from *Ulva lactuca*. **2013**, *103*, 658–661.
53. Wondwossen, M.; Op, Y.; Tesfahun, K. Photo-catalytic removal of methyl orange dye by polyaniline. **2014**, *7522*, 93–102.
54. Melaku, W.; Yadav, O.; Kebede, T. Photo-catalytic removal of methyl orange dye by polyaniline modified ZnO using Visible radiation science, technology and arts. *Journal Sci. Technol. Arts Res. J.*.**2014**, *3*, 93-102.
55. Saraswathi, V. S.; Santhakumar, K. Green Synthesis of silver nanoparticles mediated using *lagerstroemia speciosa* and photocatalytic activity against azo dye. **2017**,0–4.
56. Jayappa, M. D.; Ramaiah, C. K.; Allapuramaiah, M.; Kumar, P. Green synthesis of zinc oxide nanoparticles from the leaf, stem and in vitro grown callus of *mussaenda frondosa* l.: characterization and their applications. *J.Appl. Nanosci*. **2020**, *10*, 3057–3074.

7. APPENDIX

7.1 Appendix Figure

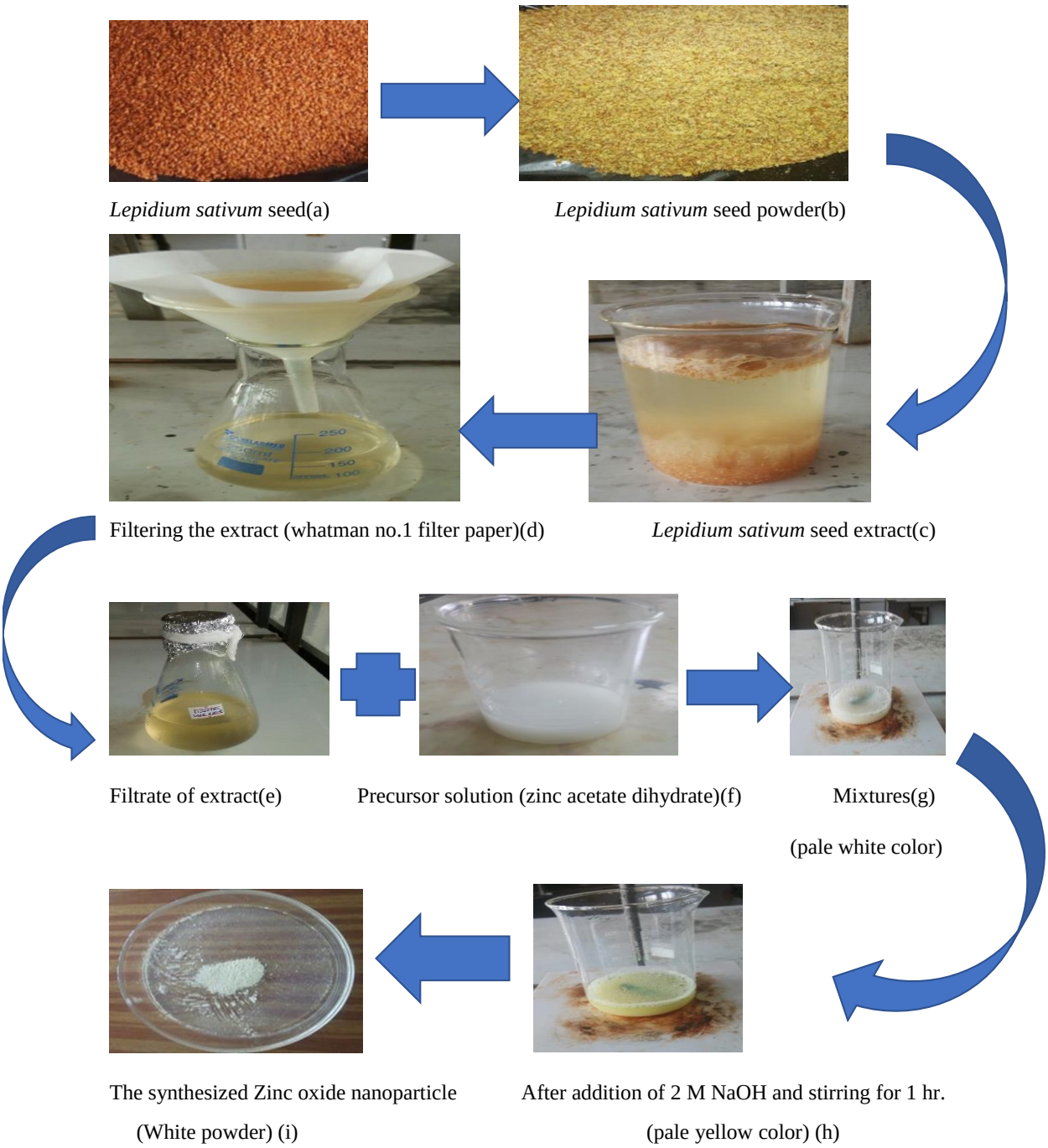

4.1.

1.A) Synthesis process of the synthesized zinc oxide nanoparticles supported *Lepidium sativum* seed extract.

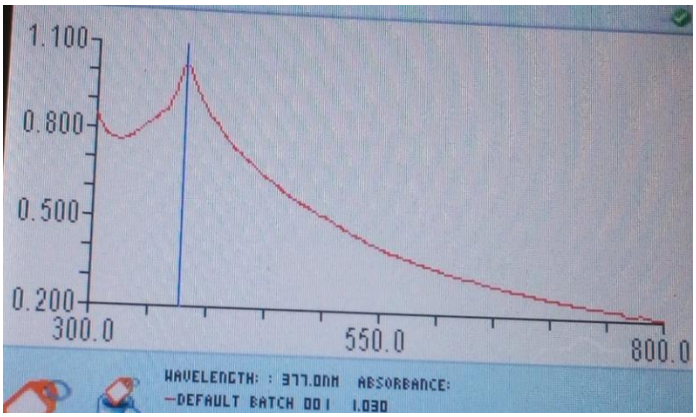

B. UV-vis spectra of as-synthesized zinc oxide nanoparticles before optimization at RT and pH 10-12.

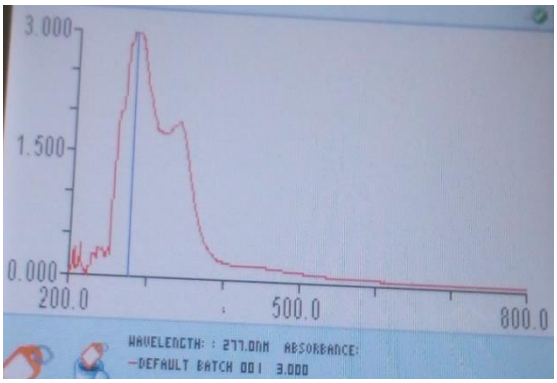

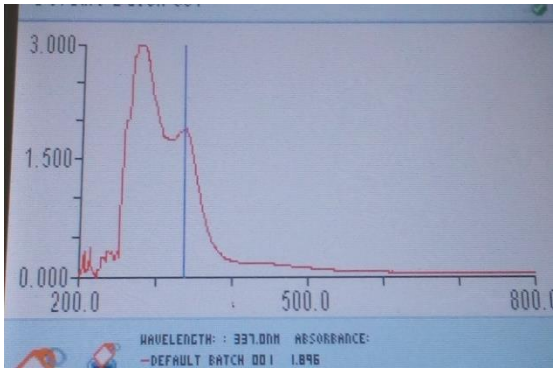

C. UV-vis spectra *Lepidium sativum* seed extract

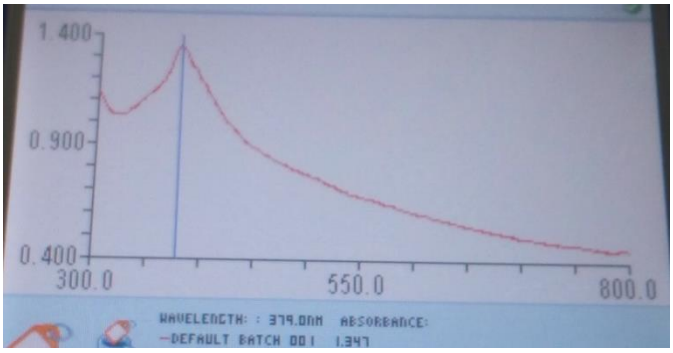

2. A: UV–Vis absorption spectra of the as-synthesized zinc oxide nanoparticles at pH of 7.

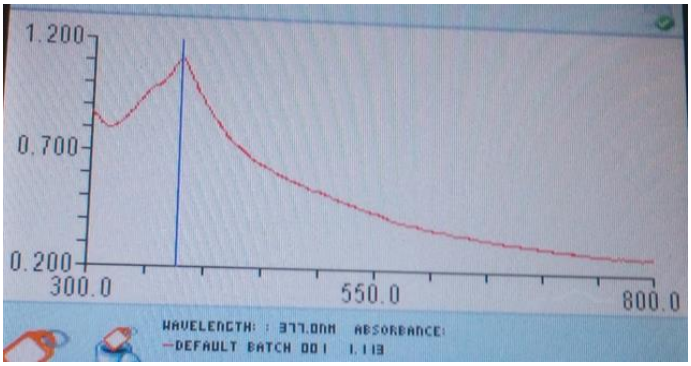

B: UV – Vis absorption spectra of the as-synthesized zinc oxide nanoparticles at pH of 8.

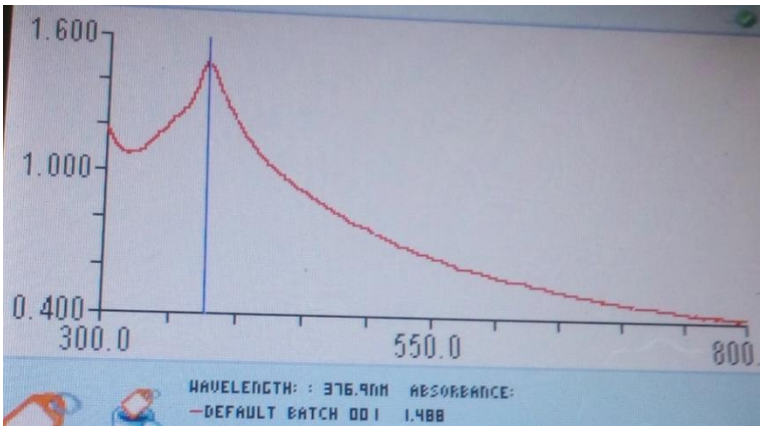

C: UV – Vis absorption spectra of the as-synthesized zinc oxide nanoparticles at pH of 10.

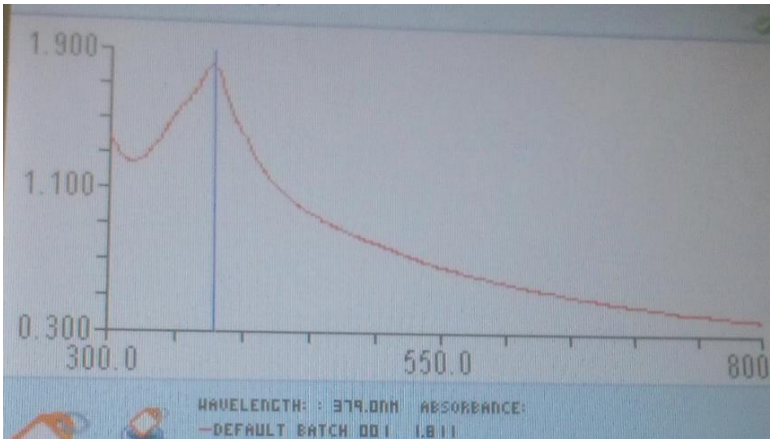

D: UV – Vis absorption spectra of the as-synthesized zinc oxide nanoparticles at pH of 12.

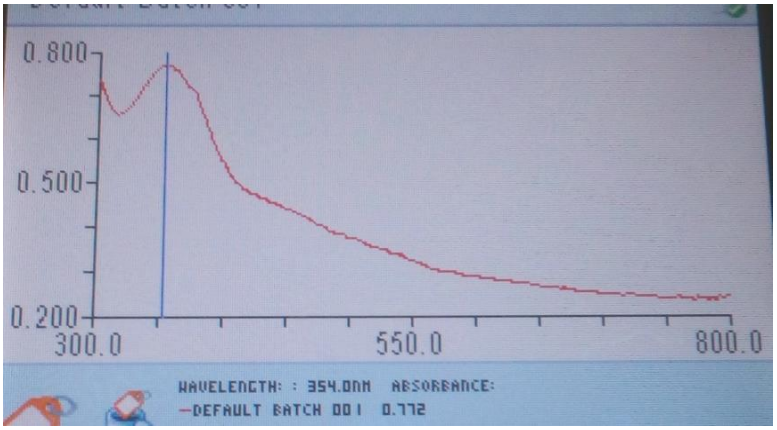

E: UV – Vis absorption spectra of the as-synthesized zinc oxide nanoparticles at pH of 14.

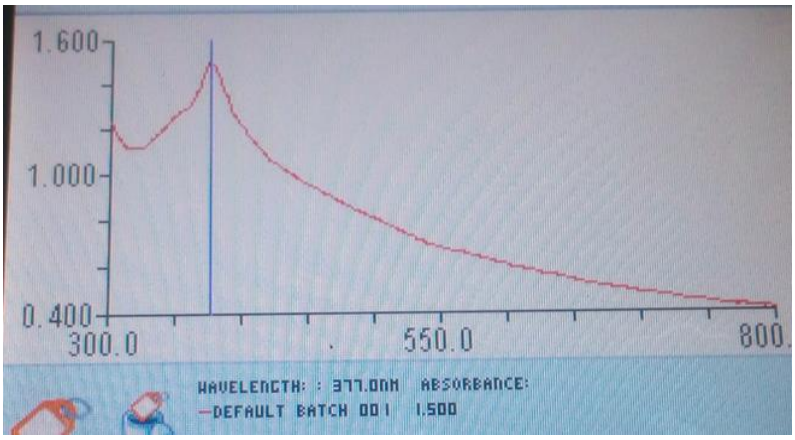

3. A: UV – Vis absorption spectra of the as-synthesized zinc oxide nanoparticles at room temperature (25 ºC).

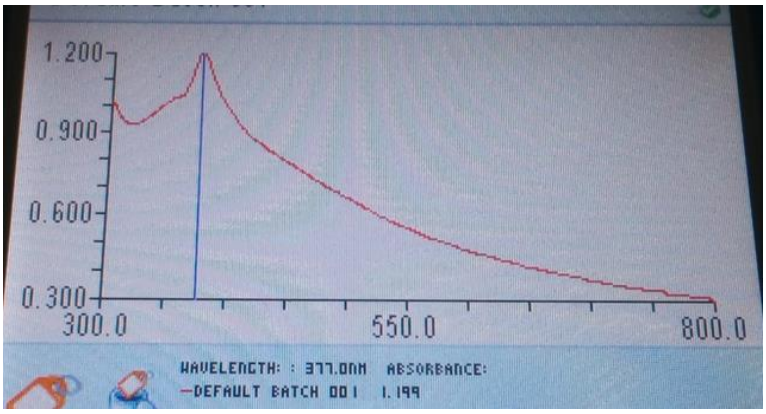

B: UV – Vis absorption spectra of the as-synthesized zinc oxide nanoparticles at temperature of 30 ºC.

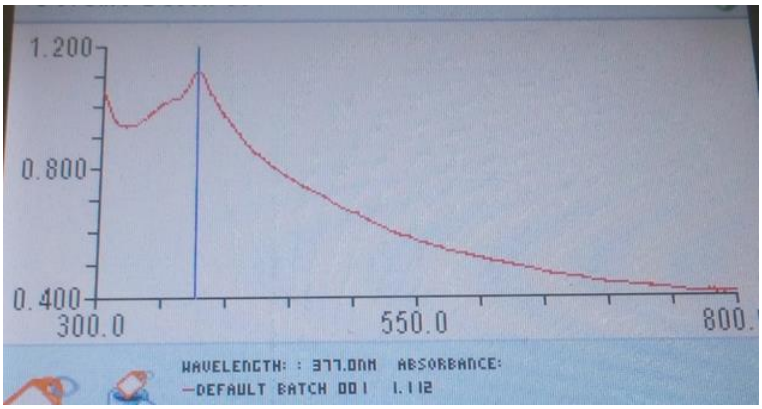

C: UV – Vis absorption spectra of the as-synthesized zinc oxide nanoparticles at temperature of 33 ºC.

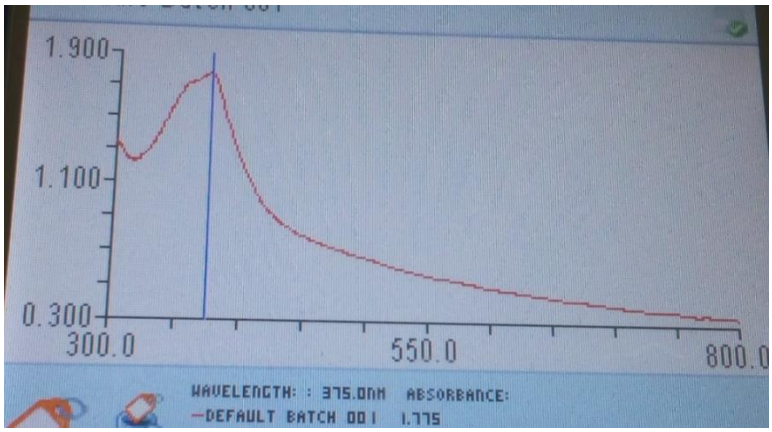

D: UV – Vis absorption spectra of the as-synthesized zinc oxide nanoparticles at temperature of 36 ºC.

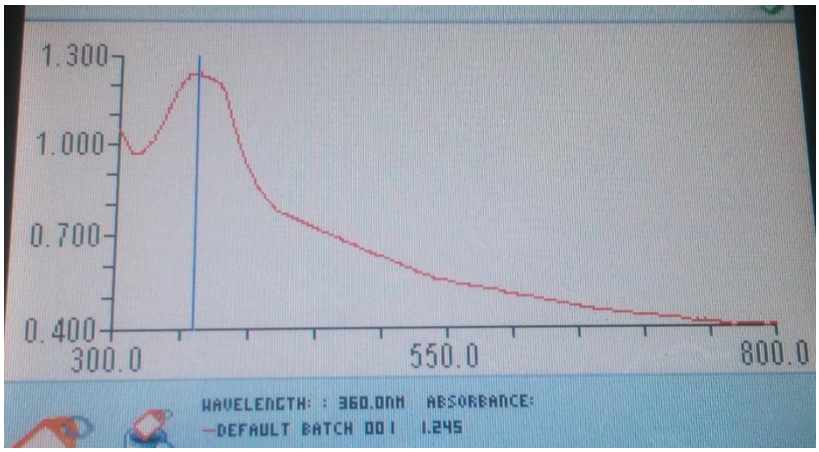

E: UV – Vis absorption spectra of the as-synthesized zinc oxide nanoparticles at temperature of 39 ºC.

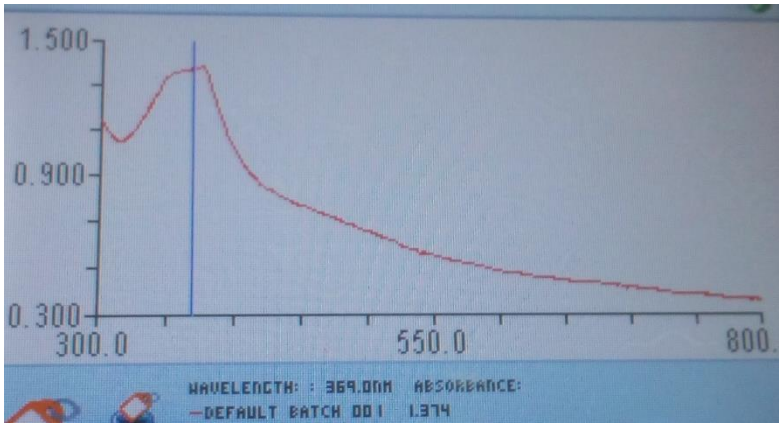

F: UV – Vis absorption spectra of the as-synthesized zinc oxide nanoparticles at temperature of 40 ºC.

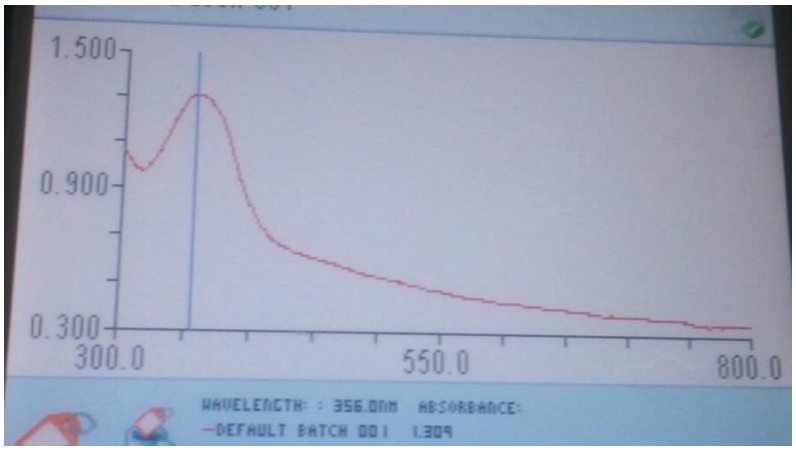

G: UV – Vis absorption spectra of the as-synthesized zinc oxide nanoparticles at temperature of 43 ºC.

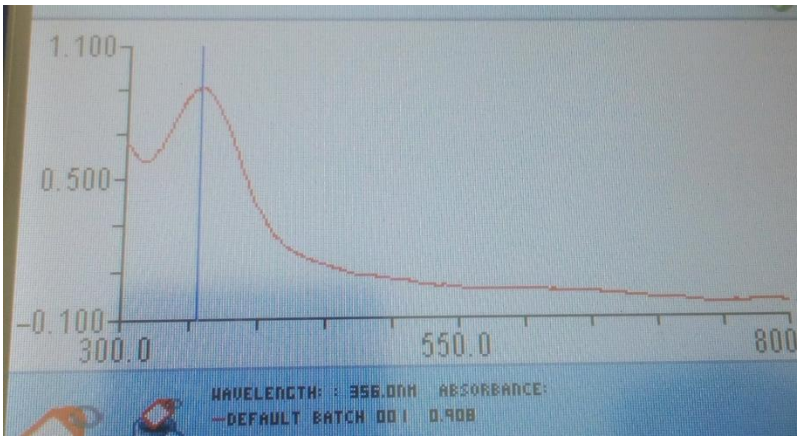

G: UV – Vis absorption spectra of the as-synthesized zinc oxide nanoparticles at temperature of 46 ºC.

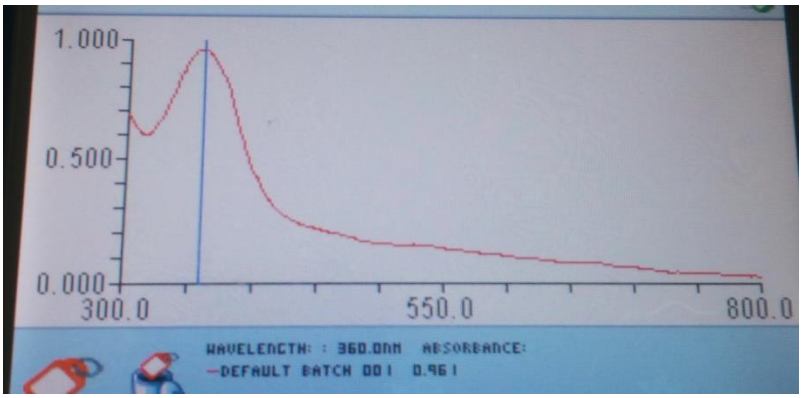

I: UV – Vis absorption spectra of the as-synthesized zinc oxide nanoparticles at 49 ºC.

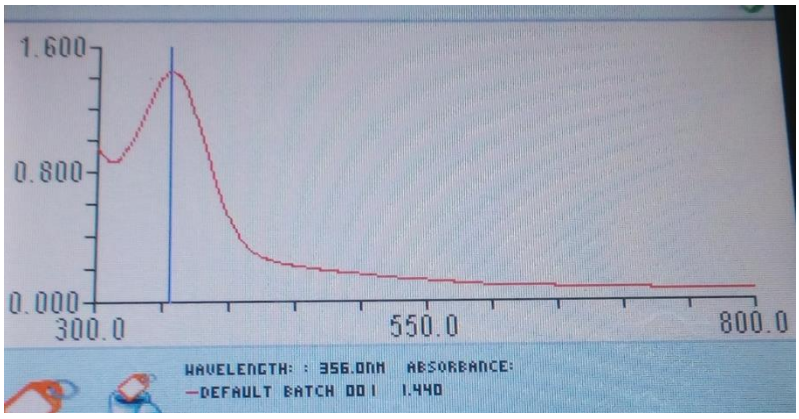

J: UV – Vis absorption spectra of the as-synthesized zinc oxide nanoparticles at temperature of 50 º.

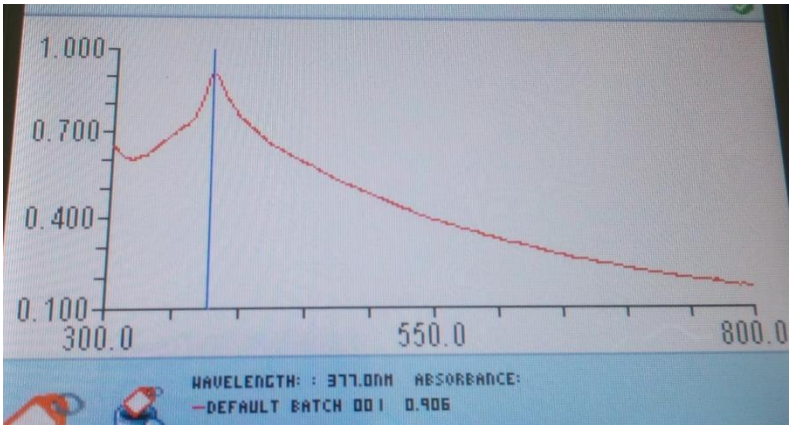

4.A: UV – Vis absorption spectra of the as-synthesized zinc oxide nanoparticles with concentration of metal ion (precursor salt solution) 0.1 M.

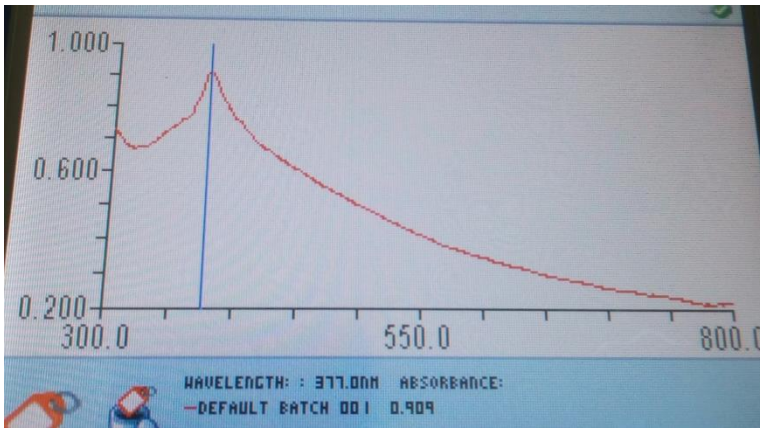

B: UV – Vis absorption spectra of the as-synthesized zinc oxide nanoparticles with concentration of metal ion (precursor salt solution) 0.05 M.

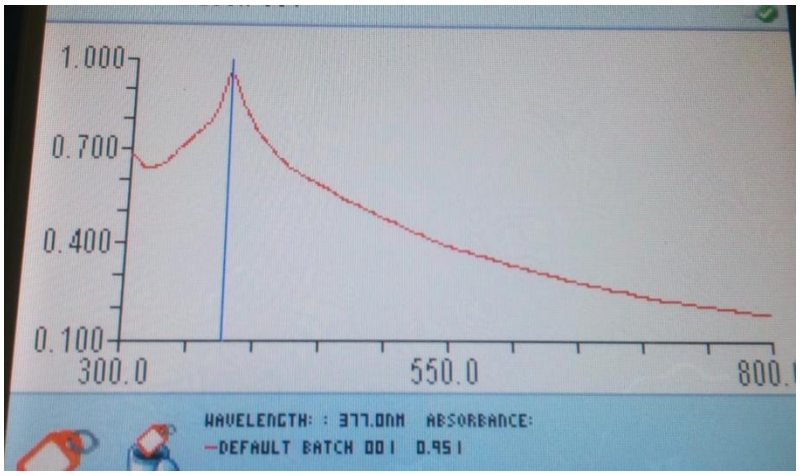

C: UV – Vis absorption spectra of the as-synthesized zinc oxide nanoparticles with concentration of metal ion (precursor salt solution) 0.046 M.

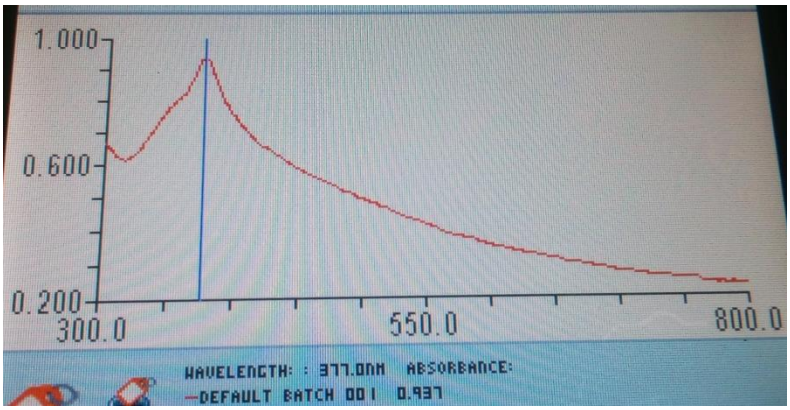

D: UV – Vis absorption spectra of the as-synthesized zinc oxide nanoparticles with concentration of metal ion (precursor salt solution) 0.025 M.

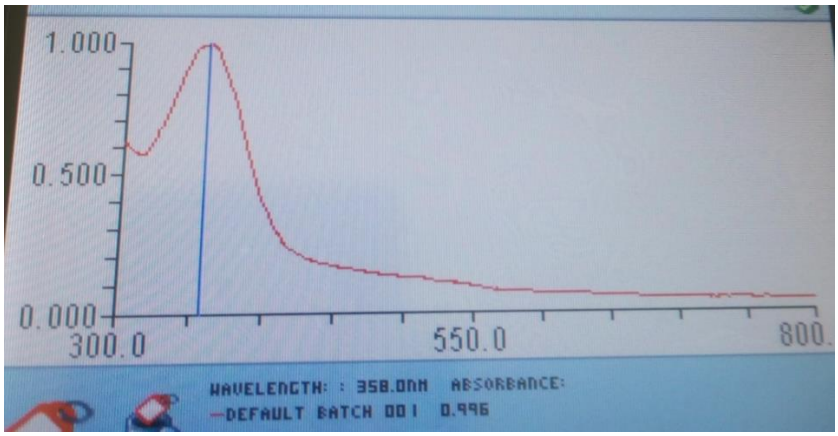

E: UV – Vis absorption spectra of the as-synthesized zinc oxide nanoparticles with concentration of metal ion (precursor salt solution) 0.01 M.

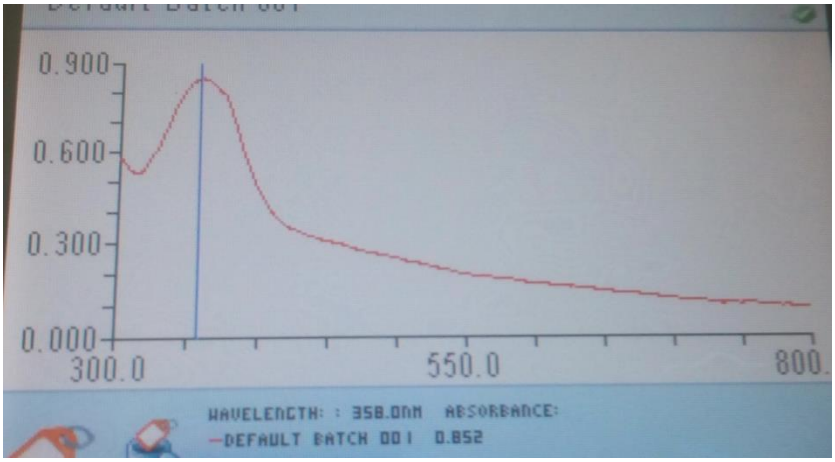

5(A): UV – Vis absorption spectra of the as-synthesized zinc oxide nanoparticles with incubation(reaction)time of 0.5 h.

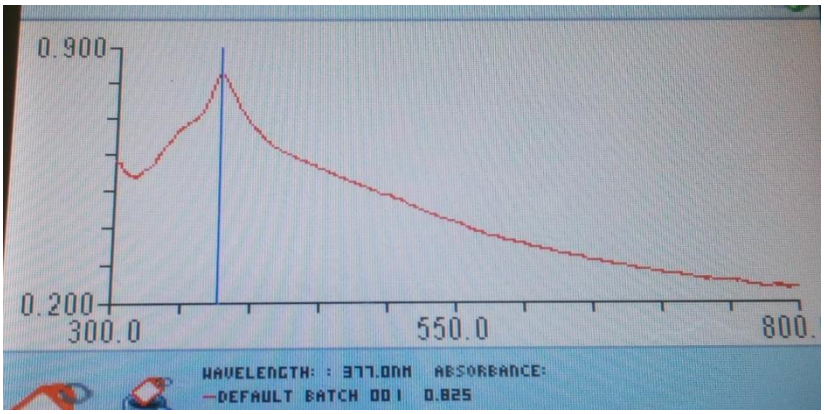

B: UV – Vis absorption spectra of the as-synthesized zinc oxide nanoparticles with incubation(reaction)time of 1 h.

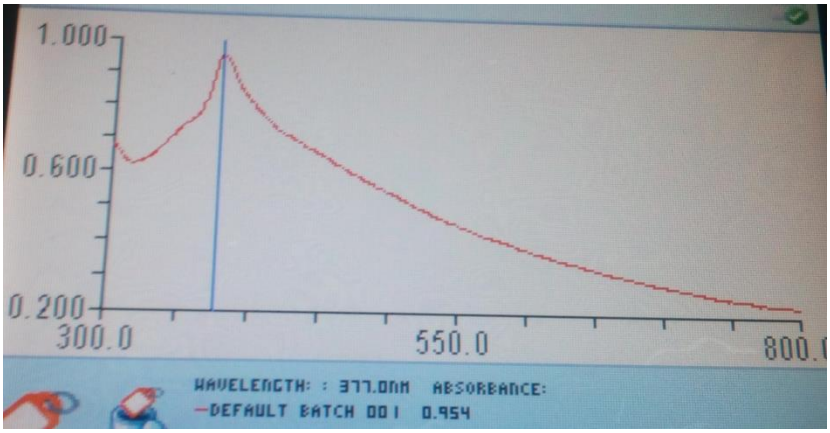

C: UV – Vis absorption spectra of the as-synthesized zinc oxide nanoparticles with incubation(reaction)time of 2 h.

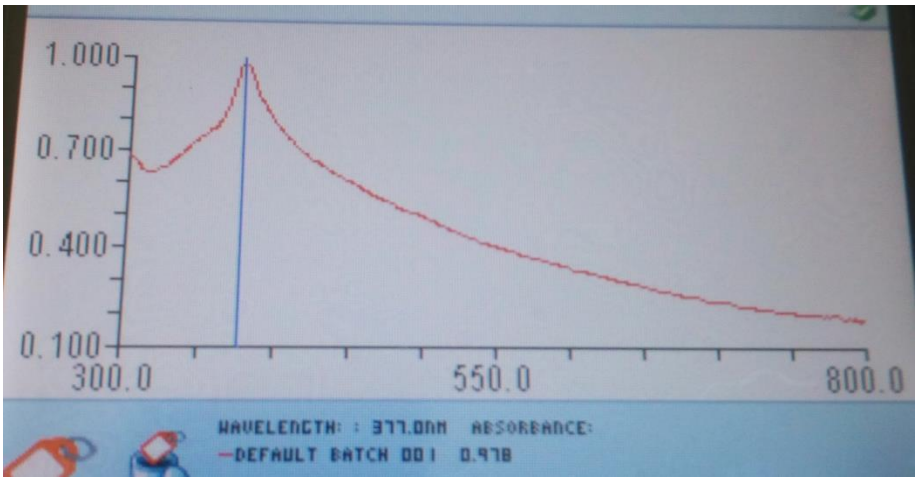

D: UV – Vis absorption spectra of the as-synthesized zinc oxide nanoparticles with incubation(reaction)time of 4 h.

In dark (a)

30 min (b)

60 min (c)

90 min (d)

180 min (g)

150 min (f)

120 min (e)

(A)

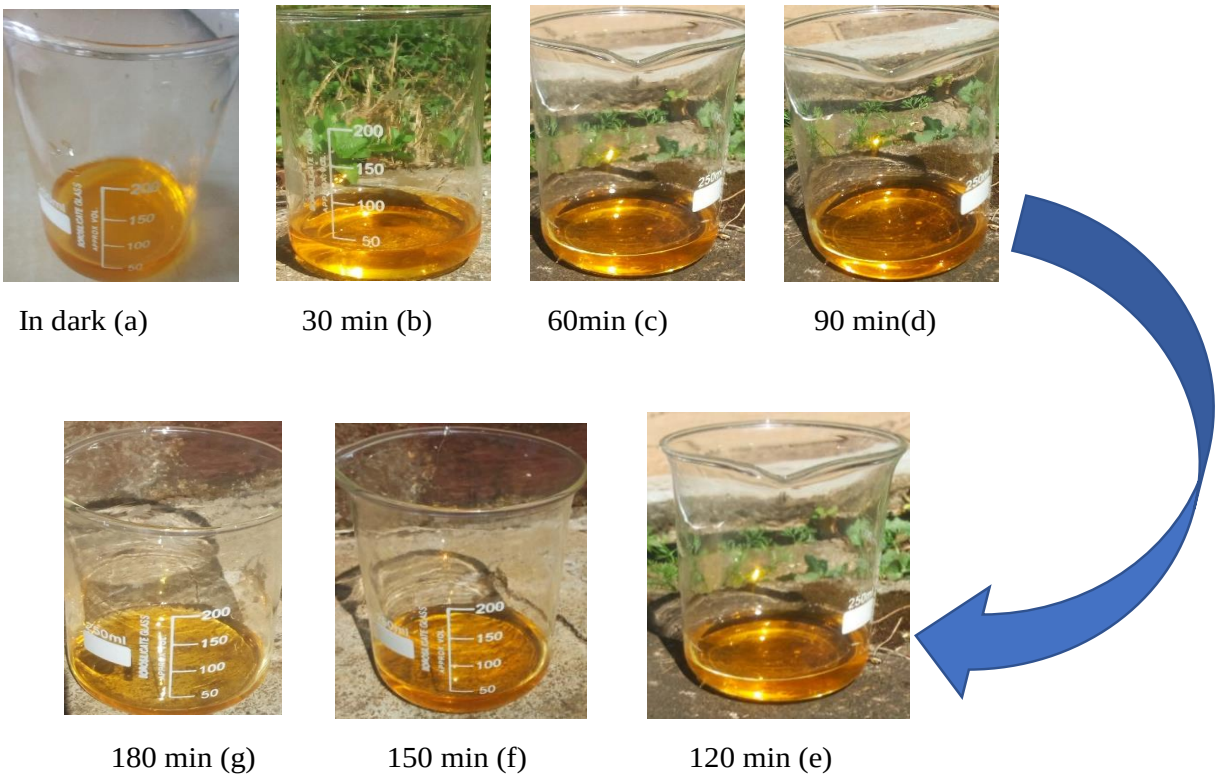

(B)

4.4

6. Optimized color change observed during photocatalytic degradation of methyl orange dye t **(A)**presence and (**B**)absence ZnO nanocatalyst in 30 min time interval.

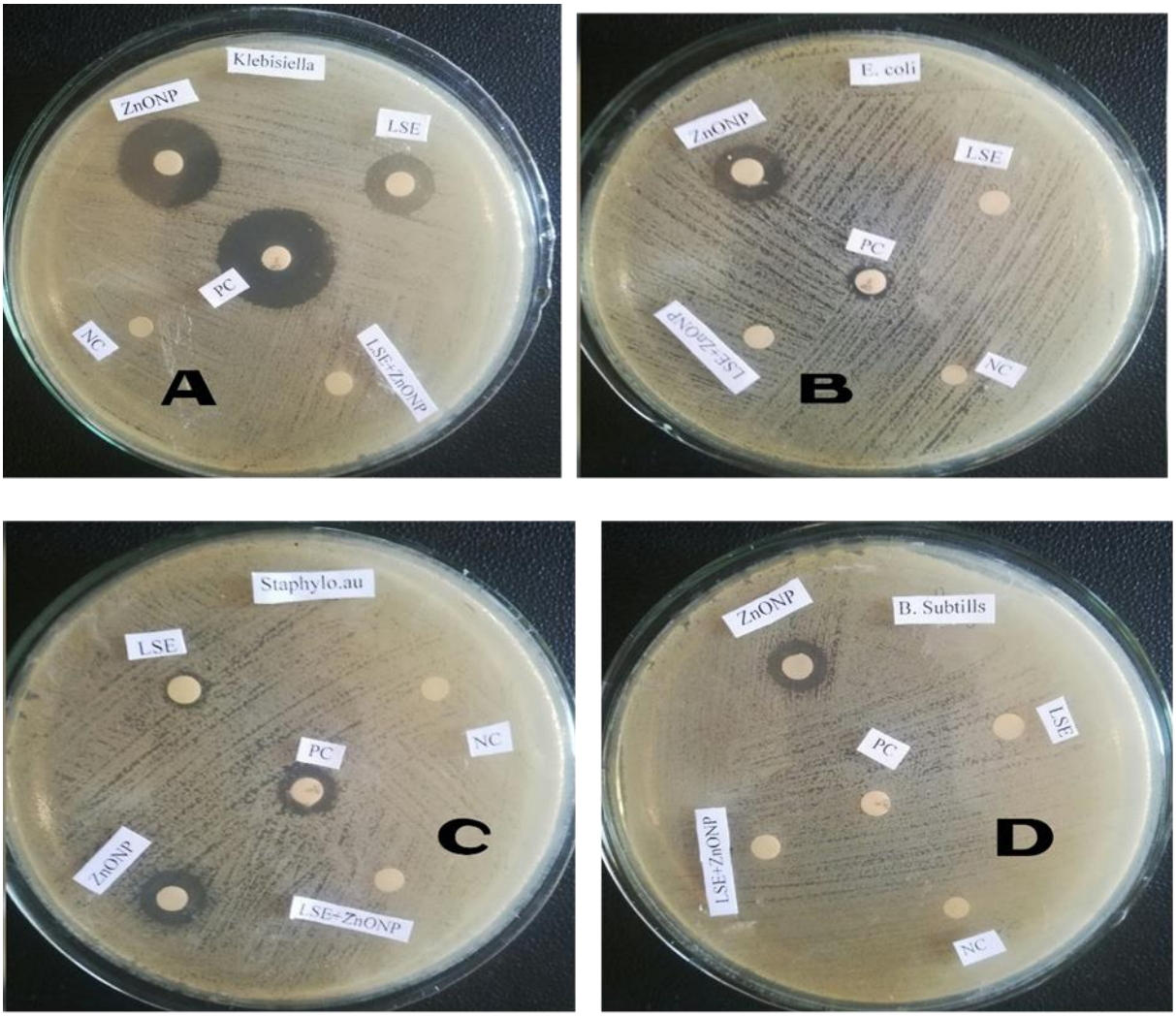

4.5.

7. Clear Zone of inhibition for antibacterial activity of ZnO NPs and plant extract for four bacterial strain with the positive control (ciprofloxacin) at the center of each Petri plate and negative control (DMSO).

A) *Klebsiella* **(B)** *Escherichia coli* **(C)** *Staphylococcus aureus* and **(D)***Bacillus subtills*